2019 Fall

"Advanced Physical Metallurgy"

- Non-equilibrium Solidification -

11.28.2019

Eun Soo Park

Office: 33-313
Telephone: 880-7221
Email: espark@snu.ac.kr
Office hours: by appointment

5.2 Methodology

5.2.1 Transformation Temperatures

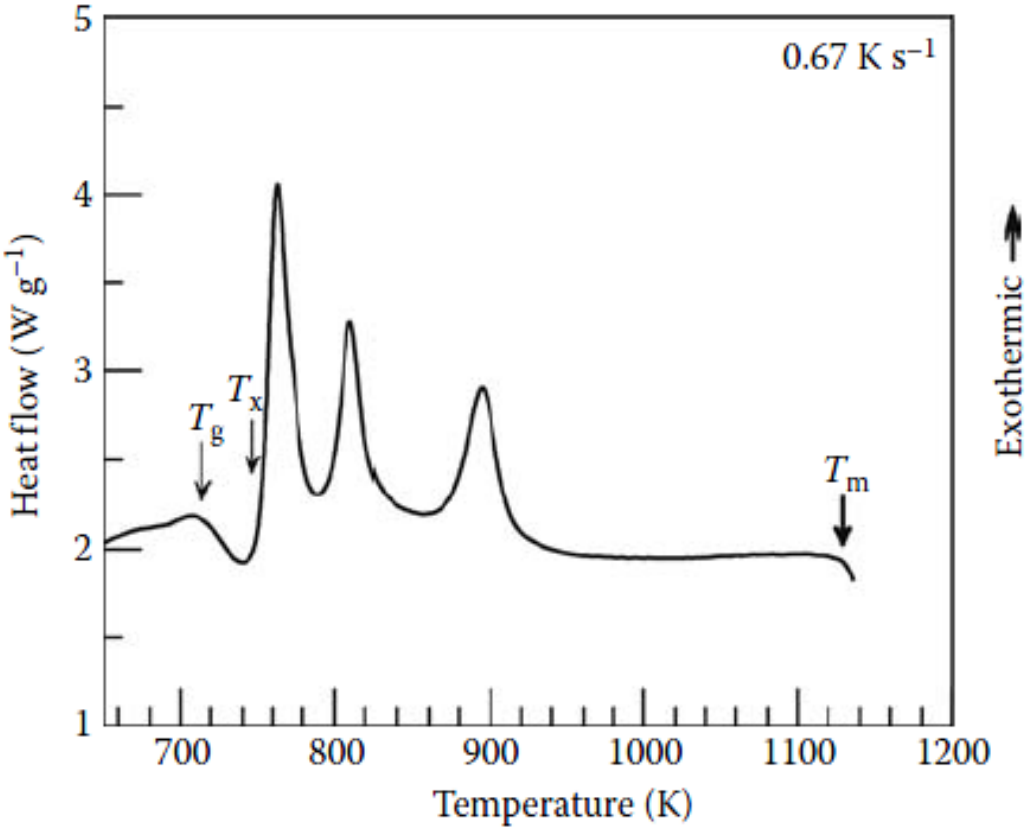

FIGURE 5.1
Schematic of a typical differential scanning calorimeter (DSC) curve obtained on heating a BMG alloy from room temperature to high temperatures at a constant heating rate of 40 K min^{-1}. Note that the curve displays three important temperatures—the glass transition temperature, T_g, the crystallization temperature, T_x, and the melting temperature, T_m. In some cases, there may be more than one crystallization temperature, depending upon the number of stages in which the glass or the supercooled liquid transforms into the crystalline phase(s).

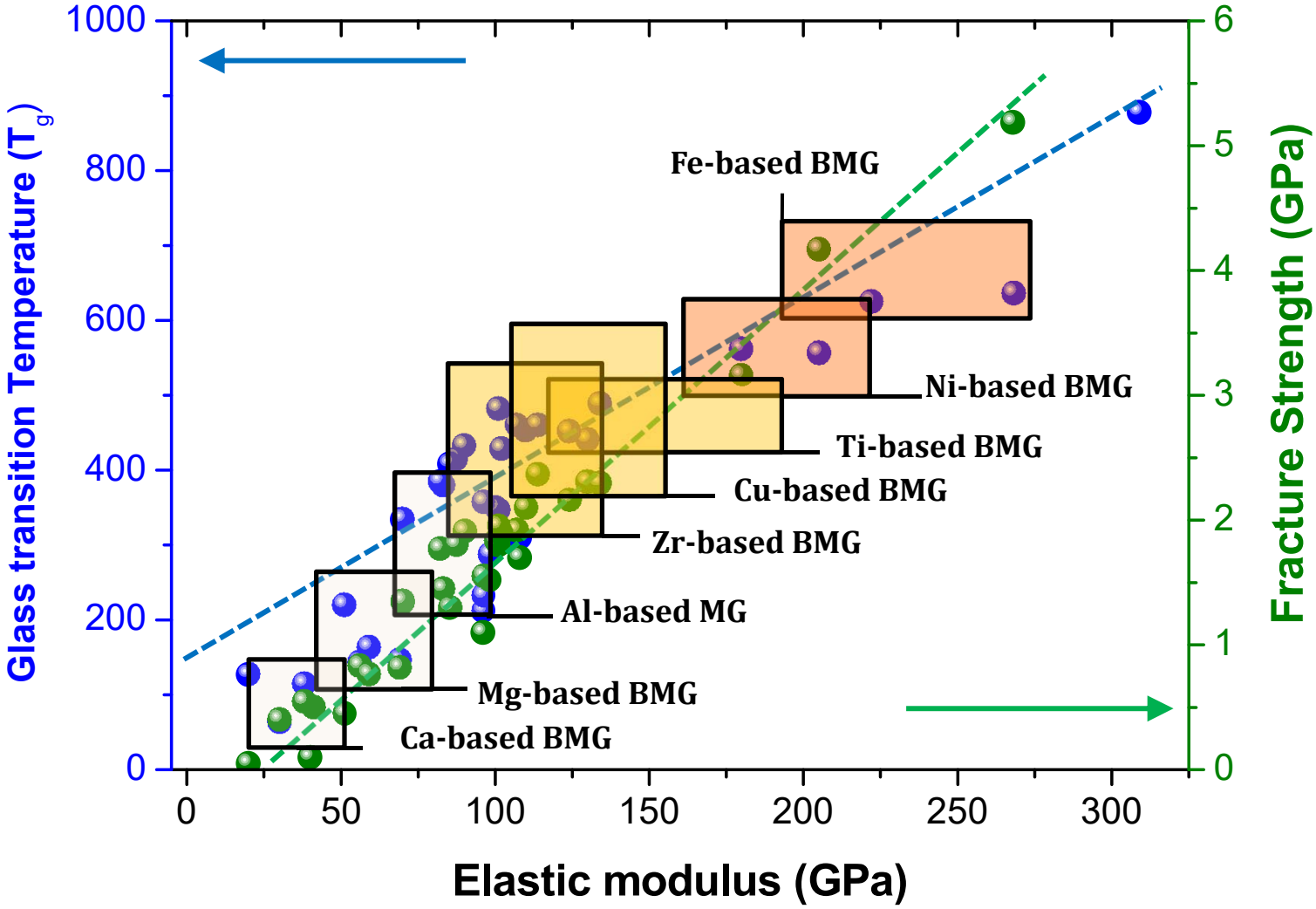
Glass transition Temperature (T_g)
Fracture Strength (GPa)
Elastic modulus (GPa)
Fe-based BMG
Ni-based BMG
Ti-based BMG
Cu-based BMG
Zr-based BMG
Al-based MG
Mg-based BMG
Ca-based BMG
0
200
400
600
800
1000
0
1
2
3
4
5
6
0
50
100
150
200
250
300

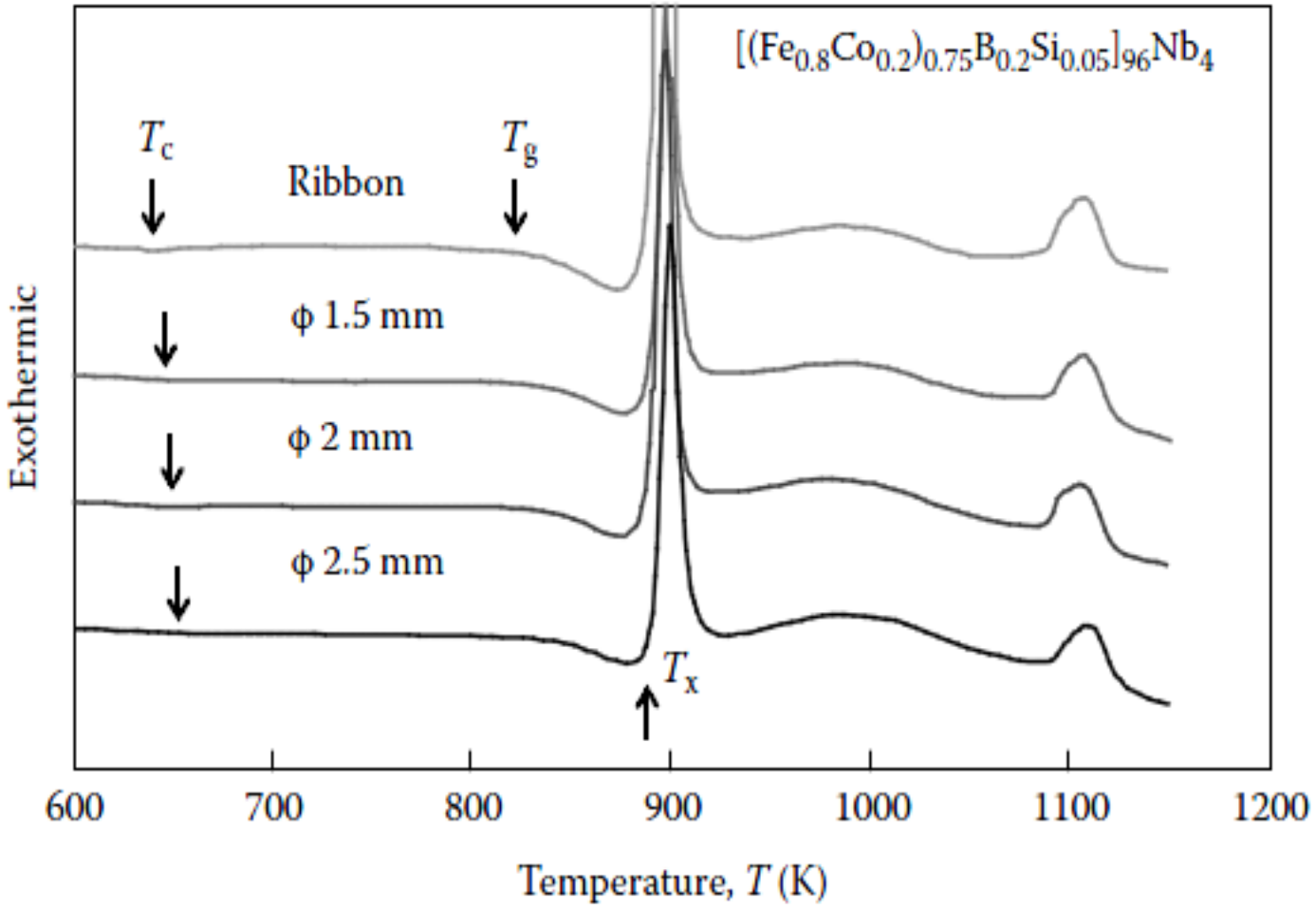

FIGURE 5.2

DSC curves of bulk glassy $[(Fe_{0.8}Co_{0.2})_{75}B_{20}Si_5]_{96}Nb_4$ alloy of different diameters (1.5, 2.0, and 2.5 mm) and melt-spun ribbon of the same composition. These curves clearly demonstrate that the transformation temperatures are identical for all the samples and that the transformation temperatures do not depend upon the diameter of the rod or the thickness of the ribbon. (Reprinted from Inoue, A. et al., *Acta Mater.*, 52, 4093, 2004. With permission.)

5.2.2 Activation energy for crystallization

Two different methods: (a) Kissinger method, (b) Ozawa method

(a) Kissinger method

$$\ln\left(\frac{\beta}{T_p^{\,2}}\right)=\left(-\frac{Q}{RT_p}\right)+A$$

where
A is a constant
R is the universal gas constant

Thus, by plotting $\ln\left(\beta/T_p^2\right)$ against $1/T_p$, one obtains a straight line whose slope is $-Q/R$, from which the activation energy for the transformation, Q can be calculated (Figure 5.3).

- Could get the required data during continuous heating in a DSC
- Possible to evaluate the individual activation energies for the nucleation and growth stages of the transformation
- May not be useful in all studies of decomposition

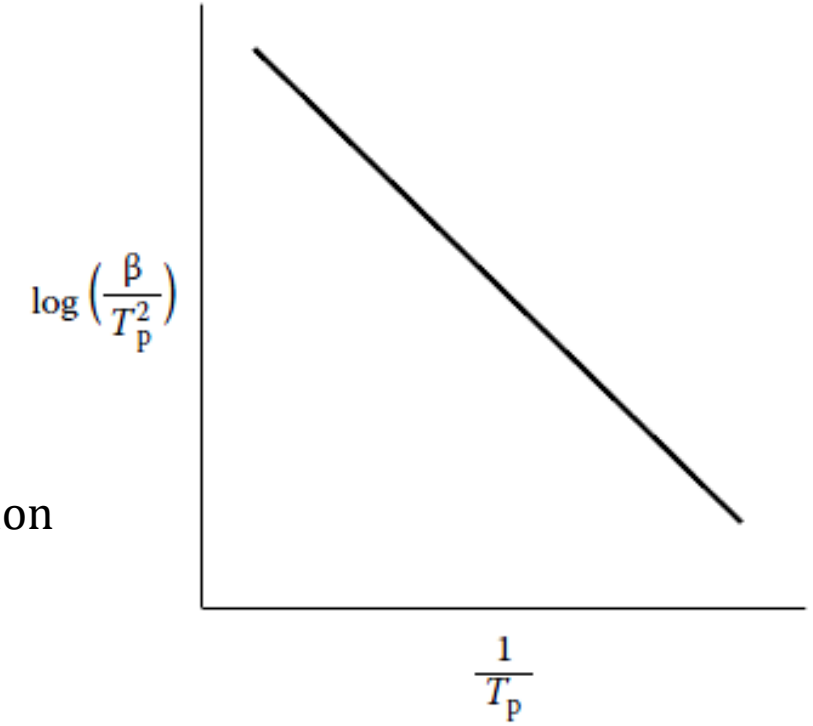

FIGURE 5.3
Kissinger plot in which $\ln(\beta/T_p^2)$ is plotted against $1/T_p$, when a straight line is obtained. The activation energy for crystallization can be calculated from the slope of this straight line.

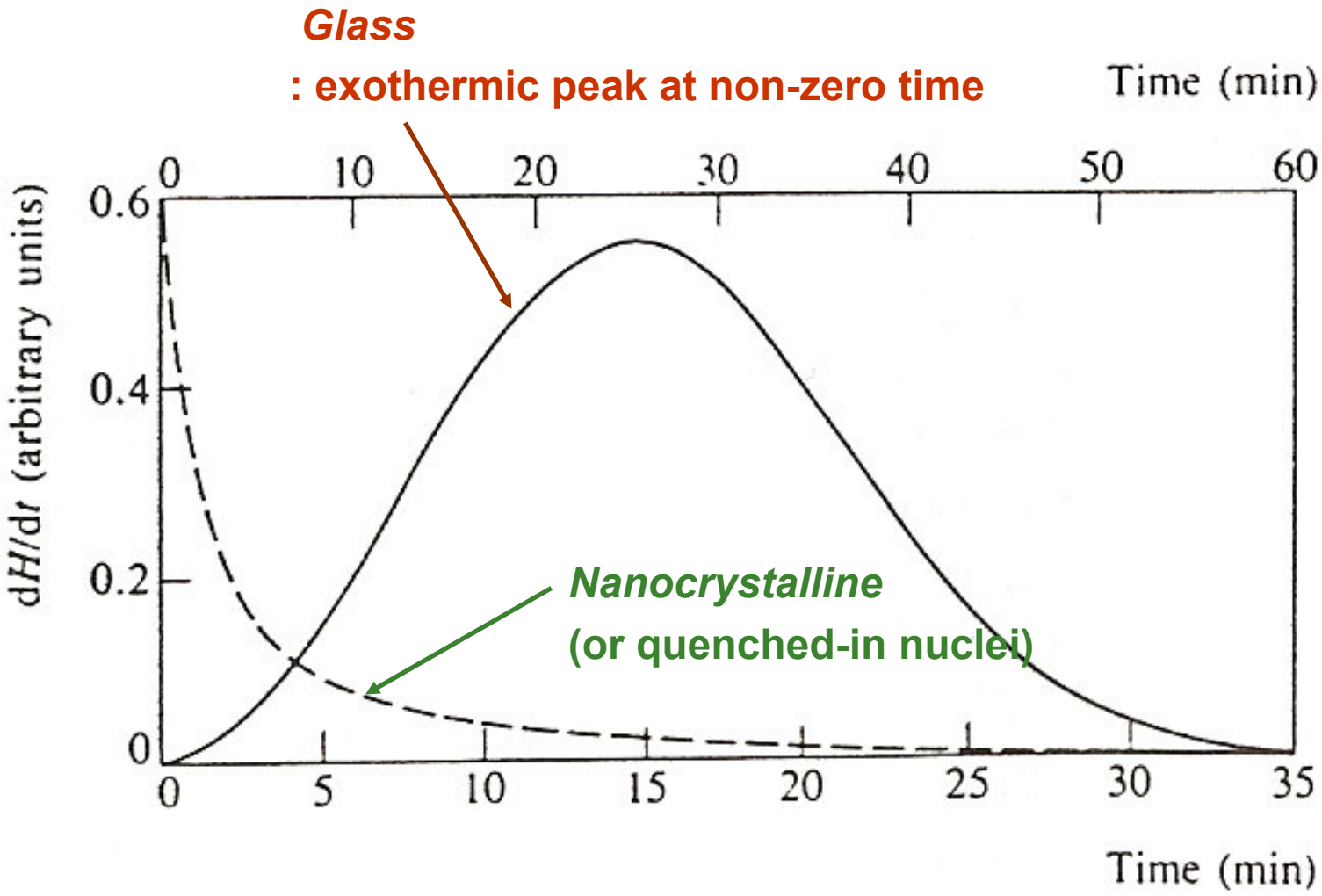

Fig. 1.4 Isothermal enthalpy release rates for crystallite nucleation and growth (solid line) and crystallite grain-coarsening mechanisms (dashed line)

5.2.3 Structural Details

- **Amorphous vs Nanocrystalline**

1) *Microstructural observation*

XRD, (HR)TEM, *EXAFS …*

2) *Thermal analysis*

DSC (Differential Scanning Calorimetry)

: Measure heat absorbed or liberated during heating or cooling

cf) **a) *glass*** → ***nucleation & growth***

(perfect random)

b) *local clustering*: quenched-in nuclei → ***only growth***

c) *Nanocrystalline* → ***growth***

5.3 Crystallization Modes in Melt-Spun Ribbons

Variables : solid solubility, number of stable & metastable intermetallic phases, composition

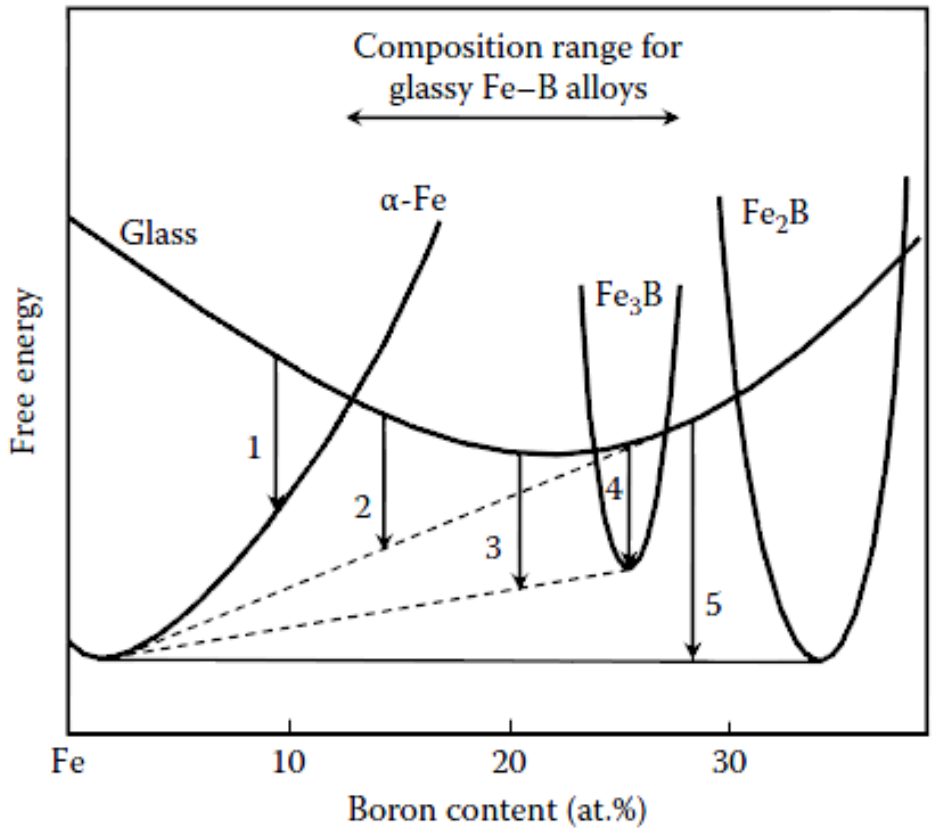

FIGURE 5.5

Hypothetical free energy vs. composition diagram for the Fe-rich Fe–B alloy system. The variation of free energy with composition is represented for the equilibrium α-Fe solid solution and the Fe_2B phases and the metastable Fe_3B phase and the glassy phase. The use of the common tangent approach will help in determining the compositions of the individual phases. The solid common tangent line represents the stable equilibrium between α-Fe and Fe_2B phases, while the dotted common tangent lines represent the metastable equilibrium between α-Fe and Fe_3B phases and α-Fe and glassy phases.

Crystallization Behaviors in Metallic Glass

Metallic glasses crystallize by a nucleation and growth process.

The driving force is the free energy difference between the glass and the appropriate crystalline phase. → (Free energy vs. Composition diagram)

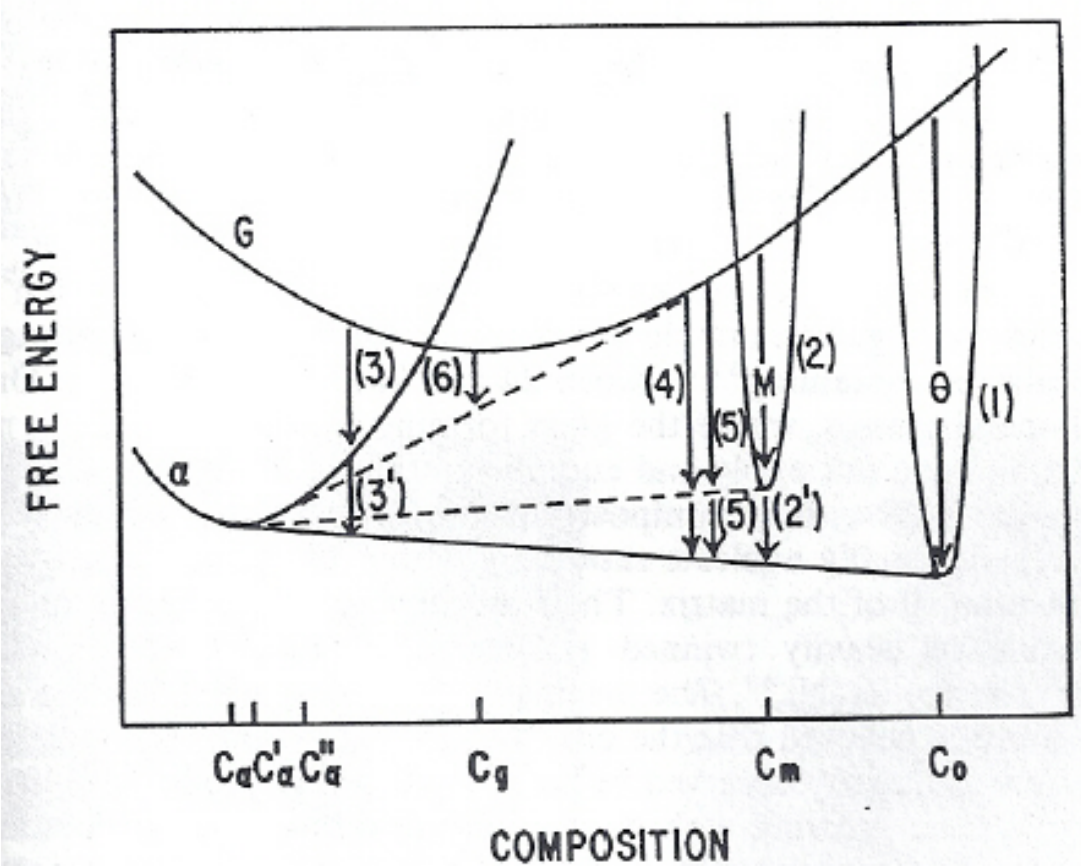

Crystallization mechanisms

1. Polymorphous Crystallization
2. Eutectic Crystallization
3. Primary Crystallization

G: Glass

α : Solid solution (Crystalline phase)

θ : Intermetallic phase

M: metastable phase

THERMODYNAMICS OF CRYSTALLIZATION

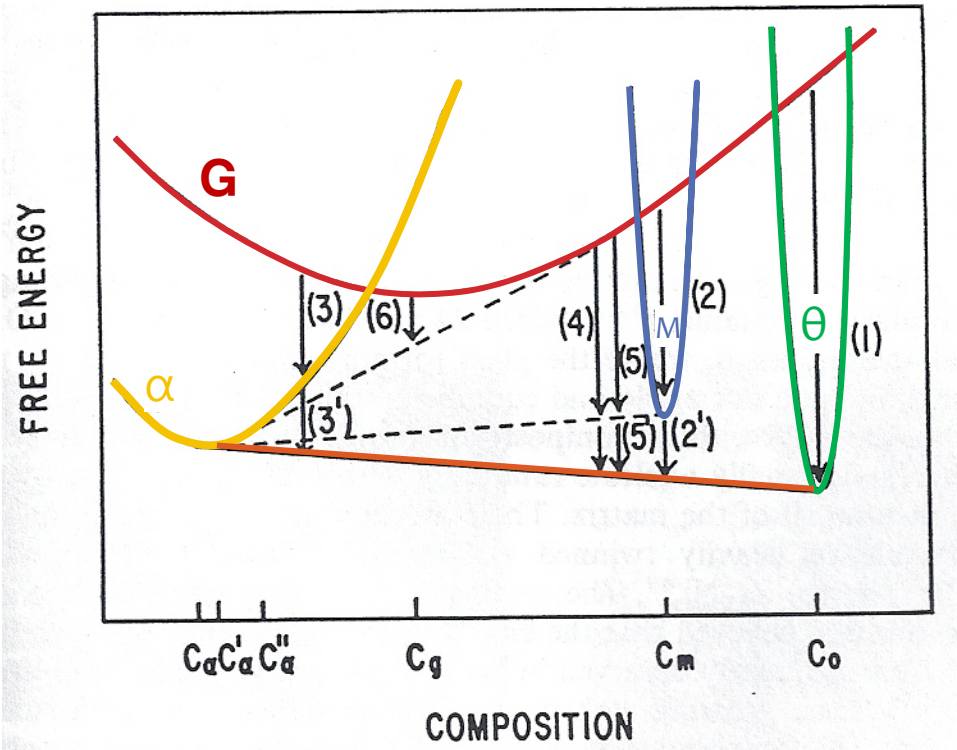

Figure 10.7 Hypothetical free energy diagram to illustrate the crystallization of a metallic glass. G, α, θ, M are respectively the free energy curves of the glass, a terminal solid solution, a stable inter-metallic phase, and a metastable phase. Stable equilibrium is indicated by the solid line; metastable equilibrium by the broken lines. The numbered arrows refer to the devitrification processes described in the text

Crystallization mechanisms

(a) Polymorphous transformation of the glass to a crystalline phase of the same composition.

The product may be either θ (1) or M(2) or a supersaturated solid solution α(3).

In the latter two cases subsequent decomposition can occur to the equilibrium mixture of α and θ (2' and 3')

1. Polymorphous Crystallization: single crystalline phase without any change in composition

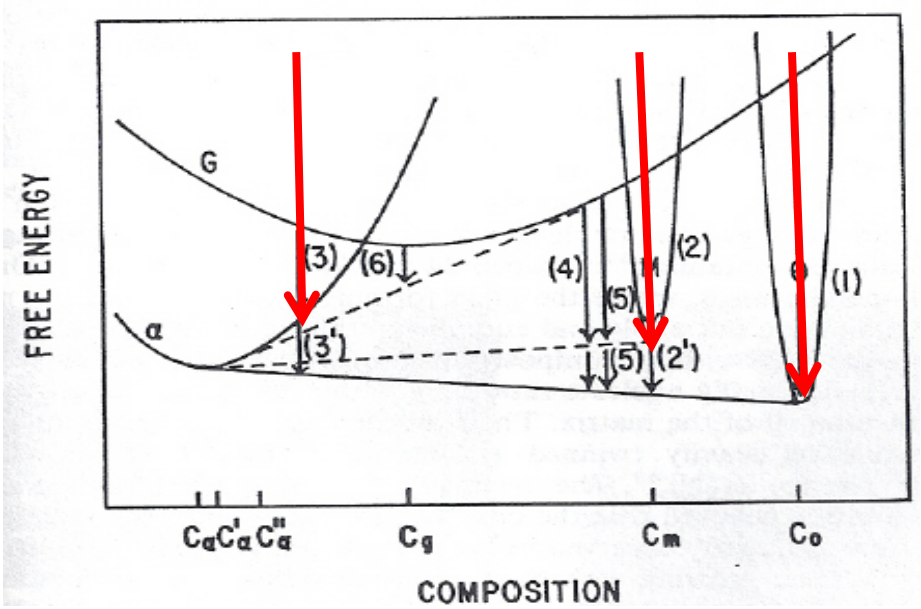

Growth rates and morphologies

$$u = a_0 v_0 \left\{ \exp\left[\frac{-\Delta F_a}{kT} \right] \right\} \left\{ 1 - \exp\left[\frac{-\Delta F_v}{kT} \right] \right\}$$

ΔF_a = activation energy for an atom to leave the matrix and attach itself to the growing phase

ΔF_v = The molar free energy difference btw C and G

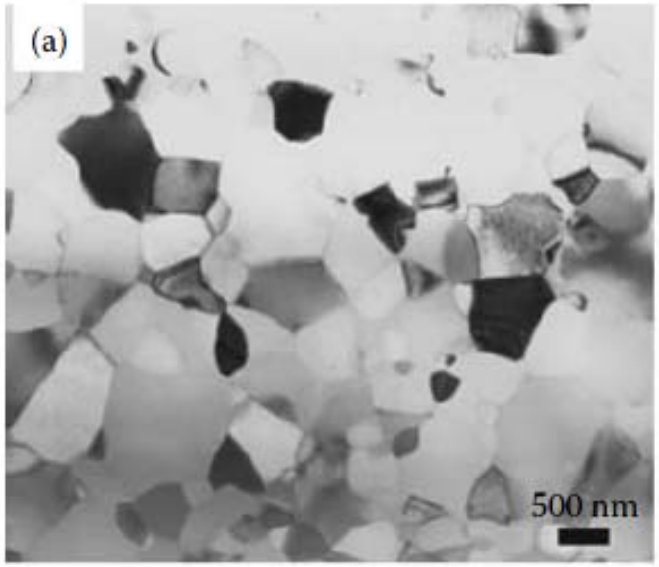

Polymorphous crystallization in a $Ti_{50}Ni_{25}Cu_{25}$ BMG alloy on annealing for 28 min at 709 K.

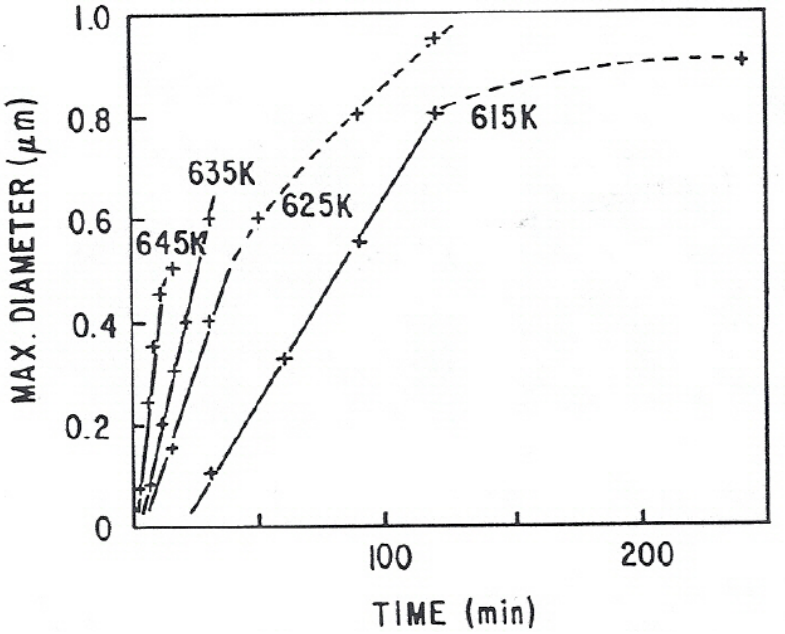

Growth kinetics of Zr_2Ni crystals in glass of same composition. The broken lines indicate crystal impingement.

THERMODYNAMICS OF CRYSTALLIZATION

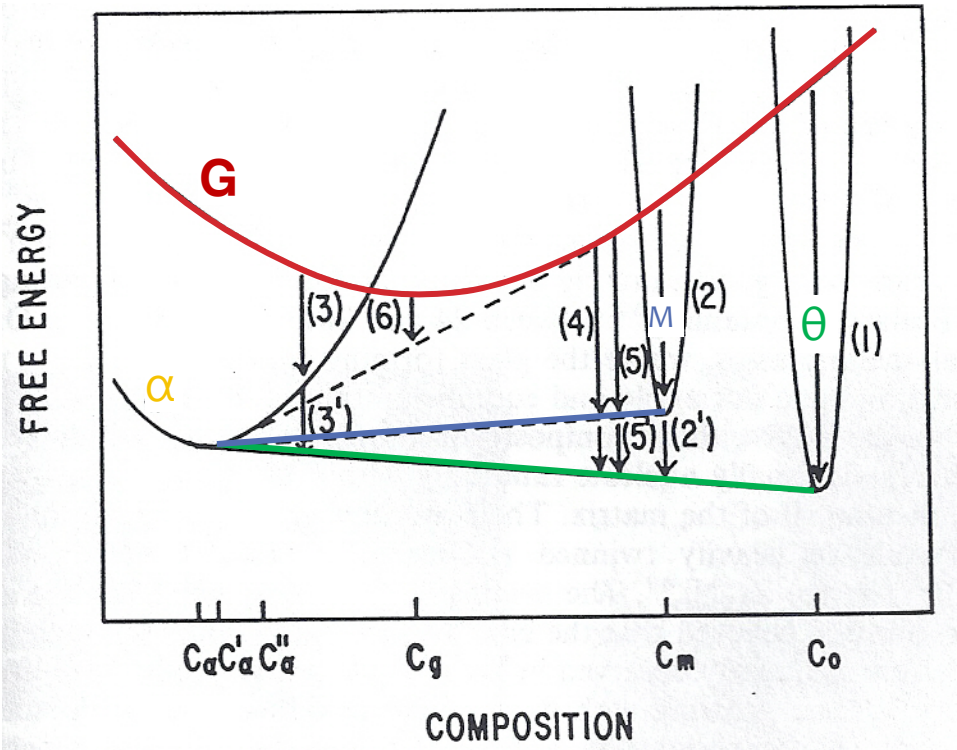

Figure 10.7 Hypothetical free energy diagram to illustrate the crystallization of a metallic glass. G, α, θ, M are respectively the free energy curves of the glass, a terminal solid solution, a stable inter-metallic phase, and a metastable phase. Stable equilibrium is indicated by the solid line; metastable equilibrium by the broken lines. The numbered arrows refer to the devitrification processes described in the text

Crystallization mechanisms

(b) Eutectic crystallization of liquids

The glass can reduce its free energy to a point on the common tangent between either α and θ (4) or α and M(5).

In the case of the metastable eutectic between α and M subsequent further decomposition to α and θ can occur. (4' and 5')

2. Eutectic Crystallization

- Largest driving force
- can occur in the whole concentration range between the stable or metastable phases (Even though the whole transformation takes place in the solid state and therefore it should be more appropriately called a eutectoid crystallization, the term “eutectic” has come to stay, presumably because the stating material (the glass) is more liquid-like.)

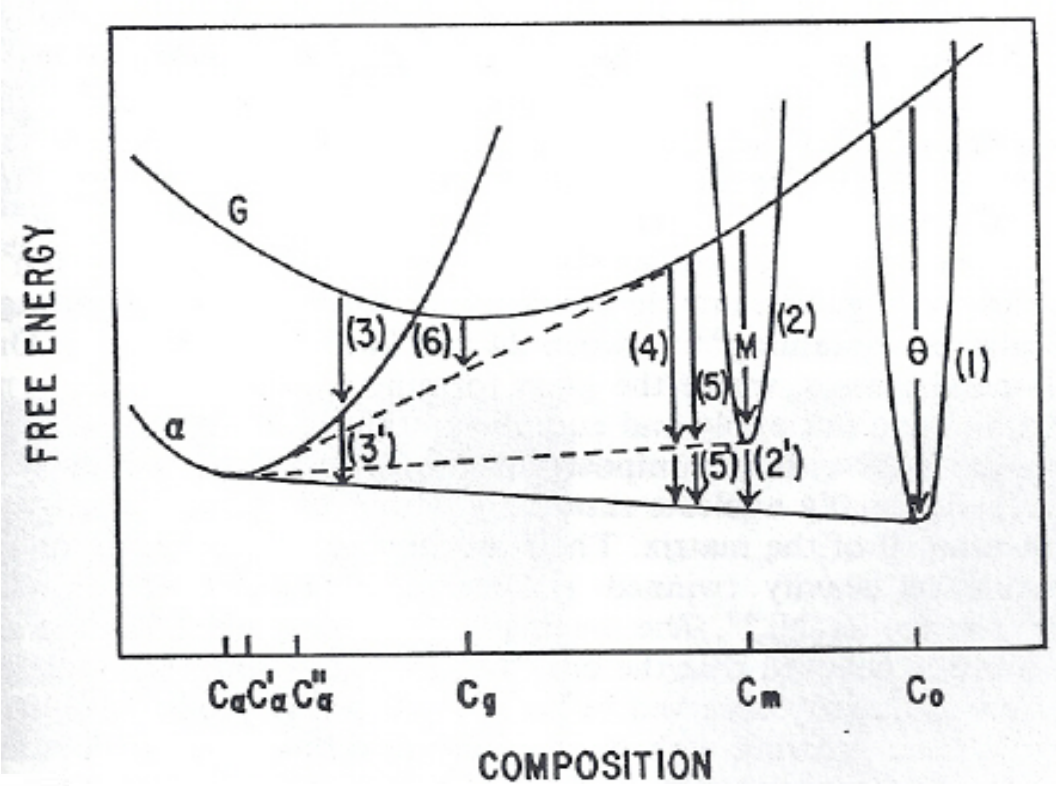

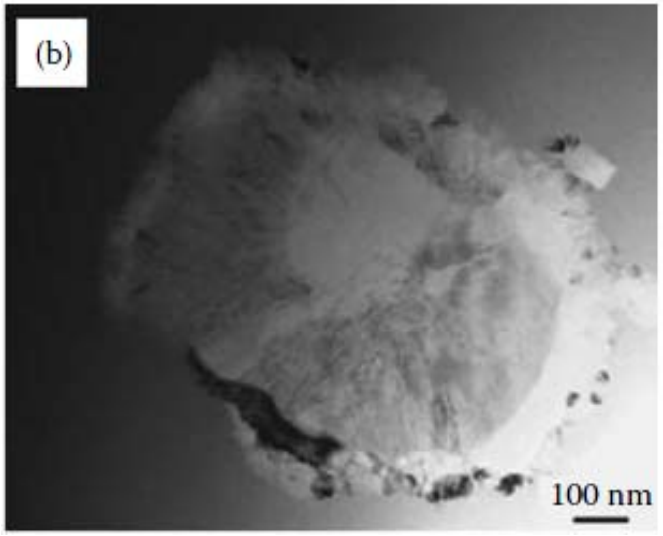

Eutectic crystallization in $Zr_{62.5}Cu_{22.5}Al_{10}Fe_5$ glassy alloy annealed for 10 min. at 713K.

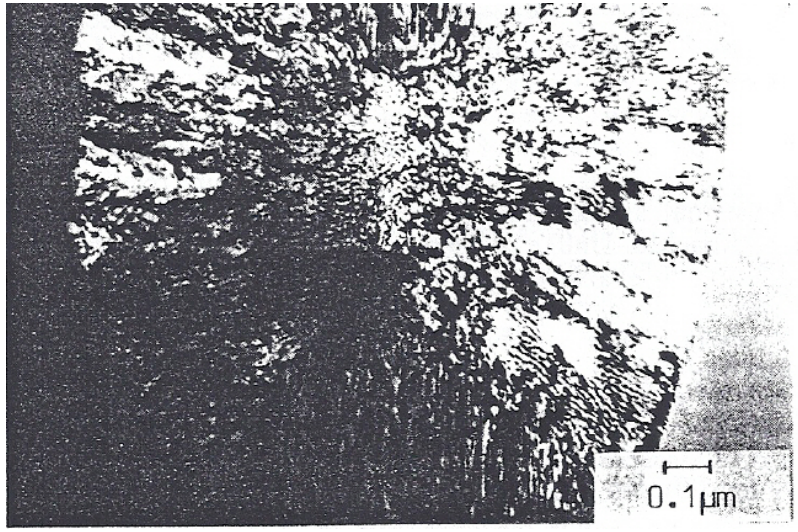

Barrel shaped eutectic crystal in $Fe_{40}Ni_{40}P_{14}B_6$ annealed for 13 min. at 385℃

THERMODYNAMICS OF CRYSTALLIZATION

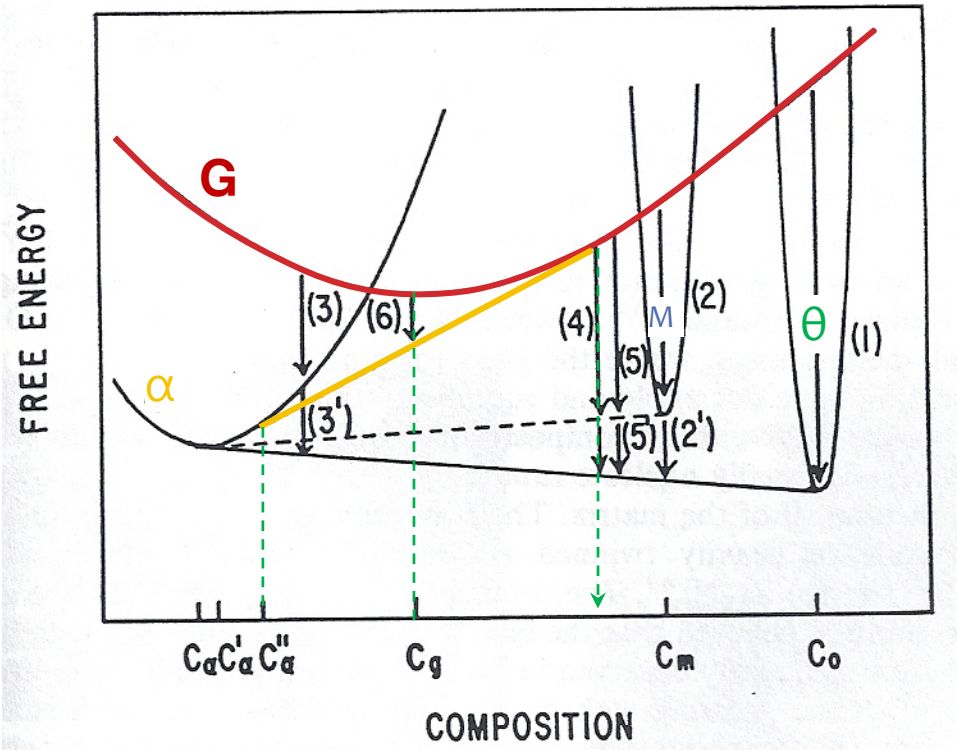

Figure 10.7 Hypothetical free energy diagram to illustrate the crystallization of a metallic glass. G, α, θ, M are respectively the free energy curves of the glass, a terminal solid solution, a stable intermetallic phase, and a metastable phase. Stable equilibrium is indicated by the solid line; metastable equilibrium by the broken lines. The numbered arrows refer to the devitrification processes described in the text

Crystallization mechanisms

(c) Primary crystallization of supersaturated solid solution (6)

Since the α has a composition c_α" which is less than that of the glass c_g solute is rejected from the growing crystals into the glass (4). Ultimately the untransformed, enriched glass (4) transforms by one of the other mechanisms discussed above.

3. Primary Crystallization

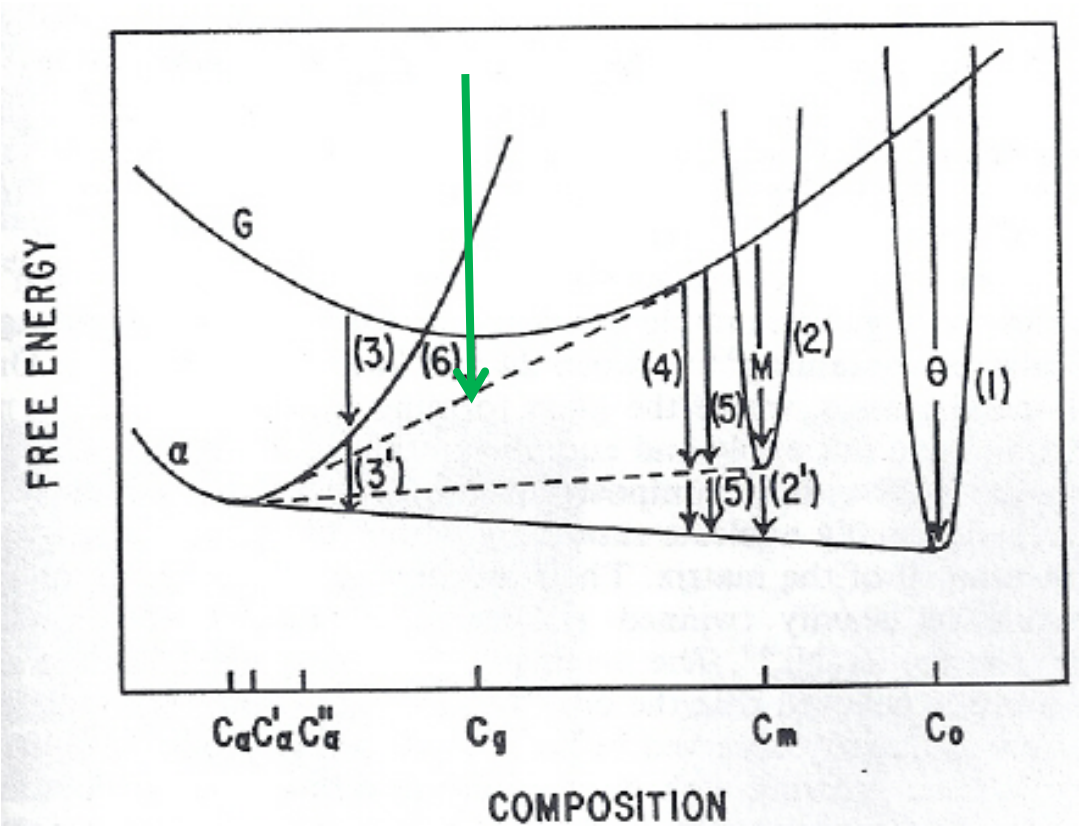

- Forms first from the glass phase
- Supersaturated solid solution
- Since the concentration of the solute in the α-Fe phase is lower than that in the glassy phase, the solute (boron) atoms are rejected into the glassy phase and consequently the remaining glass phase becomes enriched in B until further crystallization is stopped.

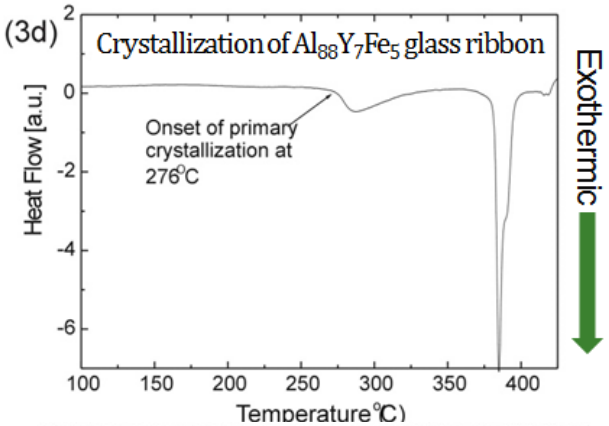

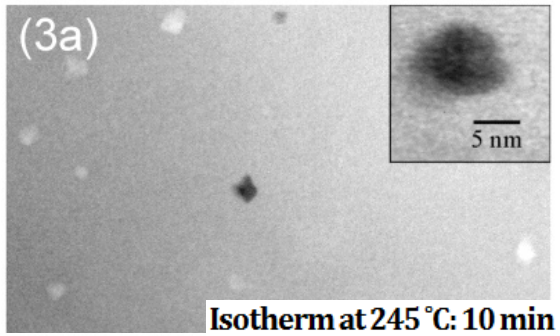

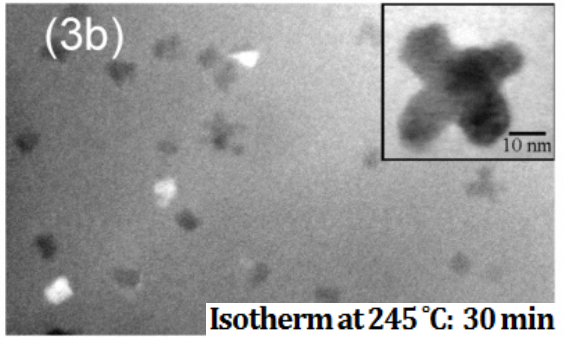

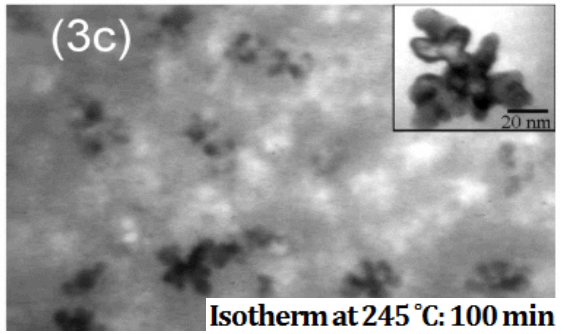

Thermodynamics of Crystallization

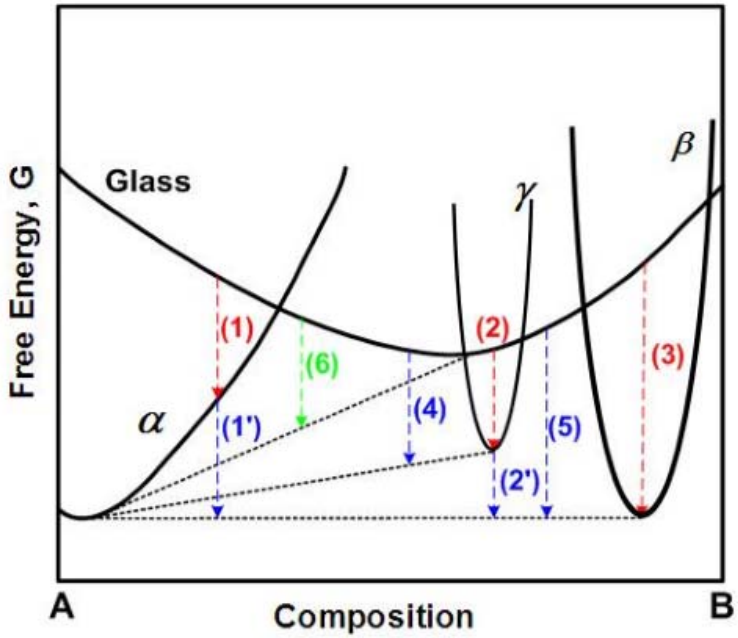

Morphology development of various crystallization reaction

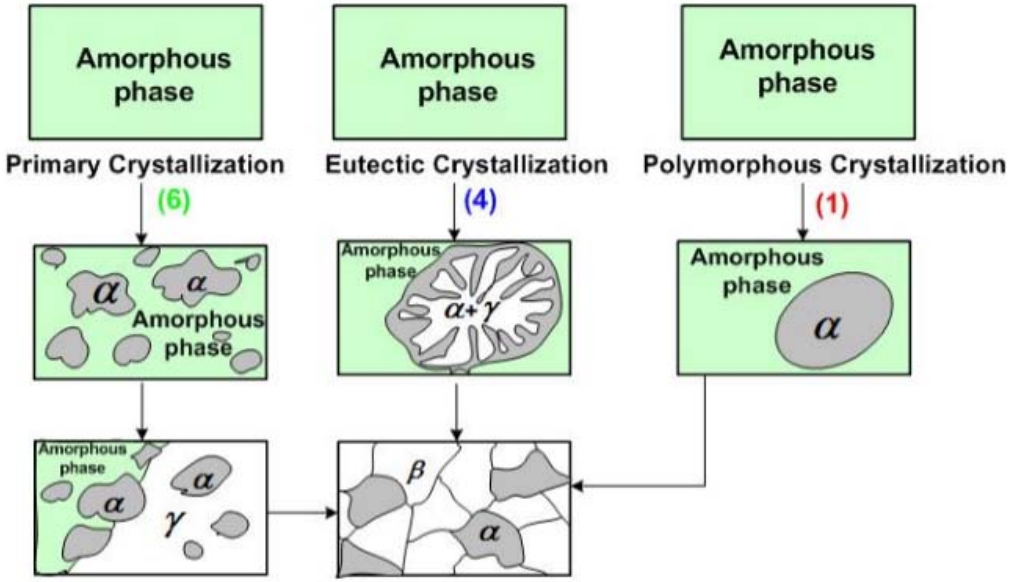

Polymorphous crystallization (1) $Am_1 \rightarrow \alpha$

Eutectic crystallization (4) $Am_1 \rightarrow \alpha+\gamma$

Primary Crystallization (6) $Am_1 \rightarrow \alpha+Am_2$

5.5. Thermal Stability of Metallic Glasses

(a) Variation of T_g and T_x in the $Zr_{65}Al_xCu_{35-x}$ (x=0, 7.5, 20) alloys

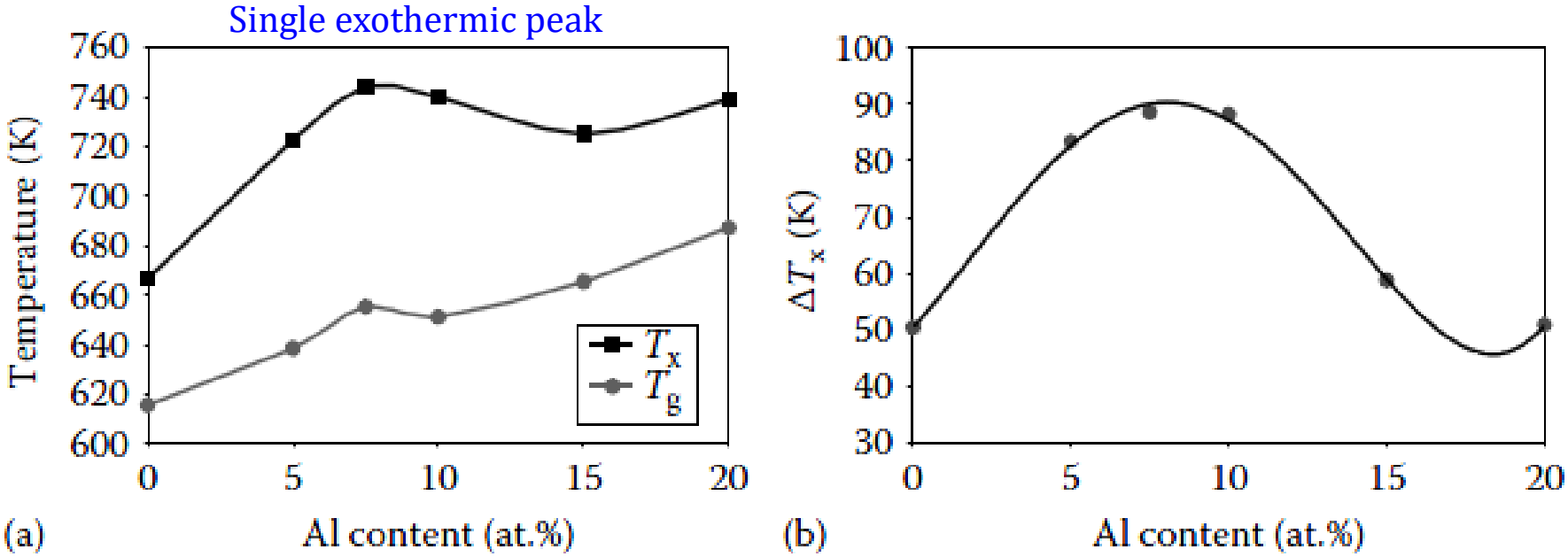

FIGURE 5.7
Variation of (a) T_g and T_x temperatures, and (b) the width of the supercooled liquid region ΔT_x (= $T_x - T_g$), with Al content in the $Zr_{65}Al_xCu_{35-x}$ glassy alloys. (Reprinted from Inoue, A. et al., *Mater. Sci. Eng. A*, 178, 255, 1994. With permission.)

5.6. Crystallization Temperatures and Their Compositional Dependence

Compositional dependence.

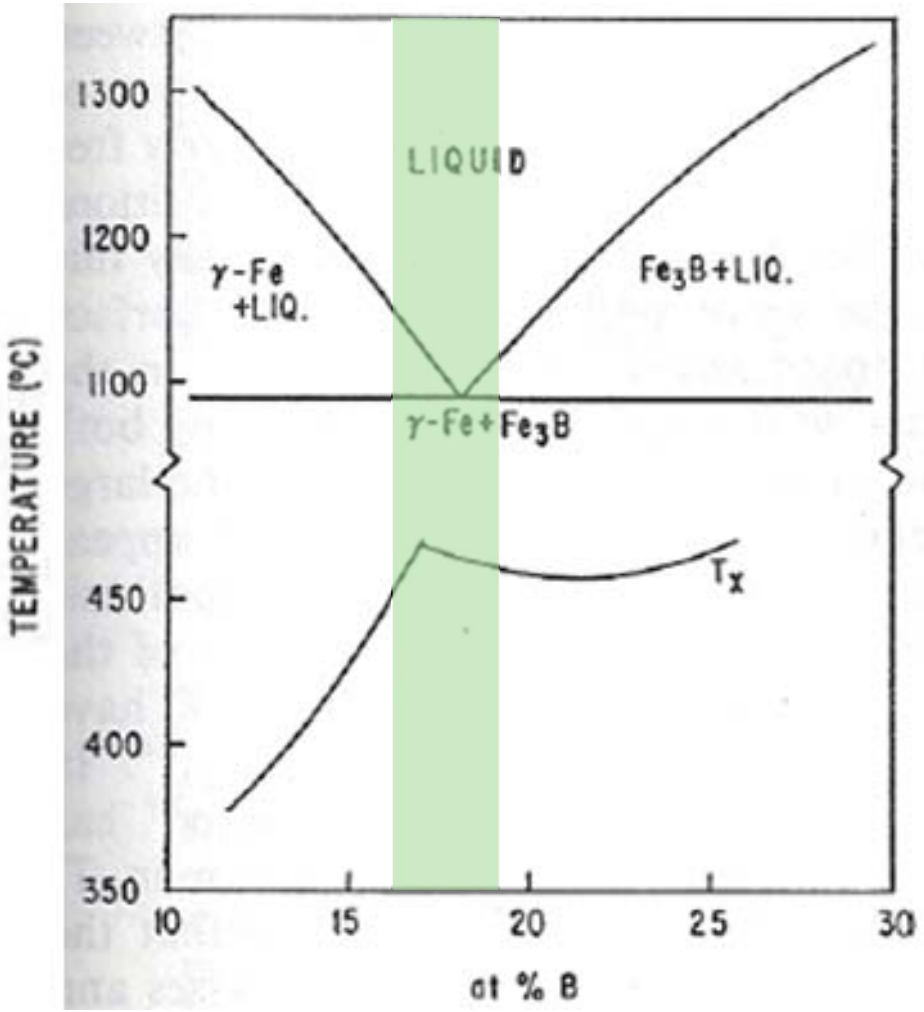

In many binary

Metal-Metalloid glass (Fe-B)

T_x is a maximum near the eutectic composition

→ The same does not appear to be the case in all-metallic glasses

Metal-Metal glass (Ni-Zr)

A monotonic decrease of T_x with increasing Zr content despite the existence in two eutectics

5.6. Crystallization Temperatures and Their Compositional Dependence

Compositional dependence.

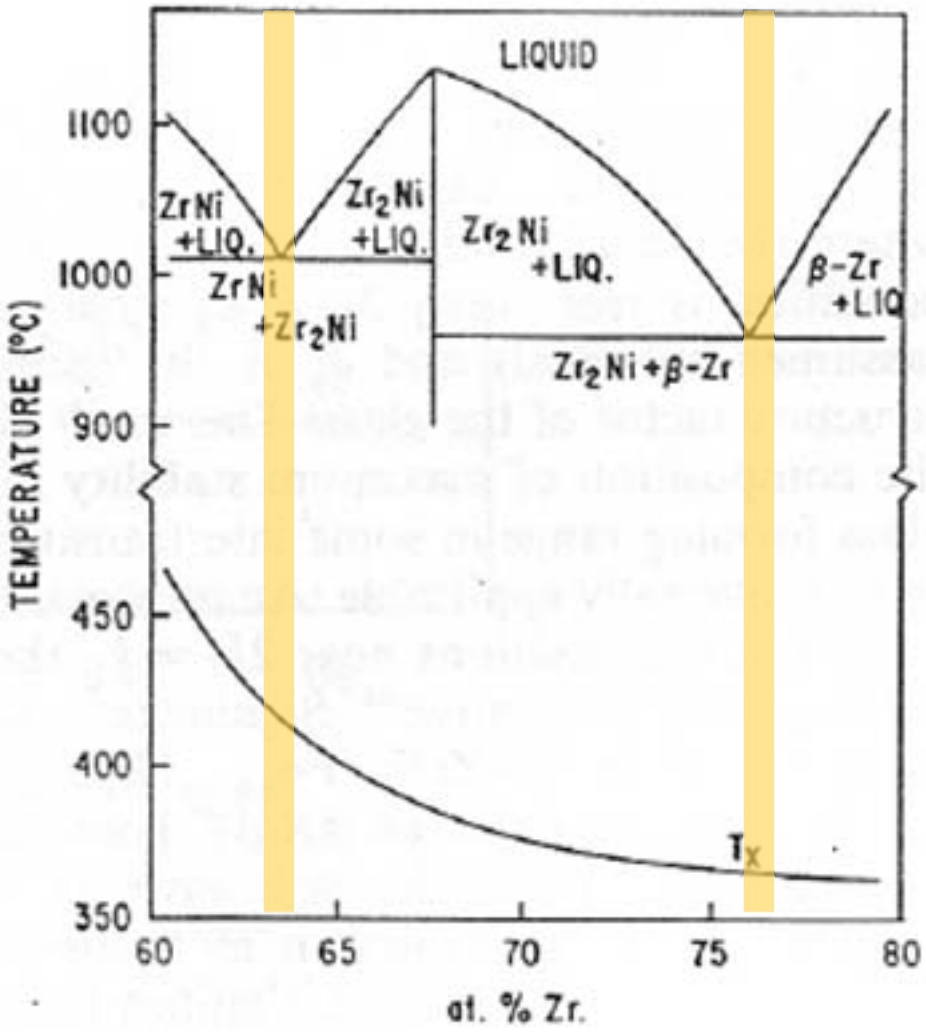

In many binary

Metal-Metalloid glass (Fe-B)

Tx is a maximum near the eutectic composition

→ The same does not appear to be the case in all-metallic glasses

Metal-Metal glass (Ni-Zr)

A monotonic decrease of T_x with increasing Zr content despite the existence in two eutectics

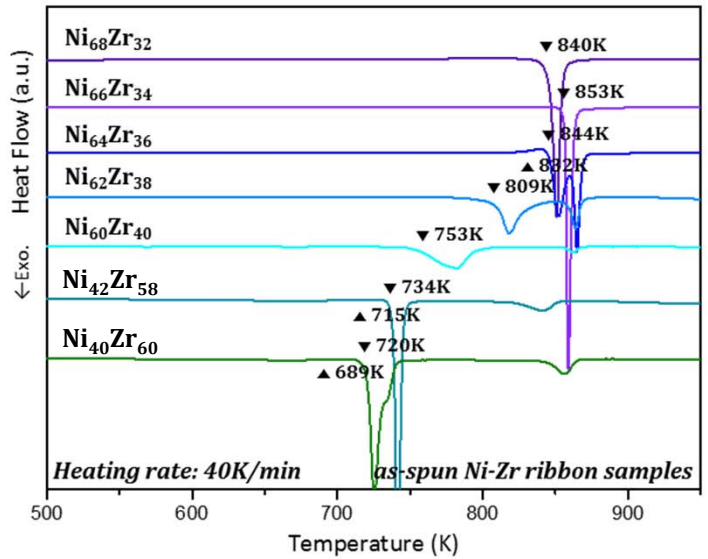

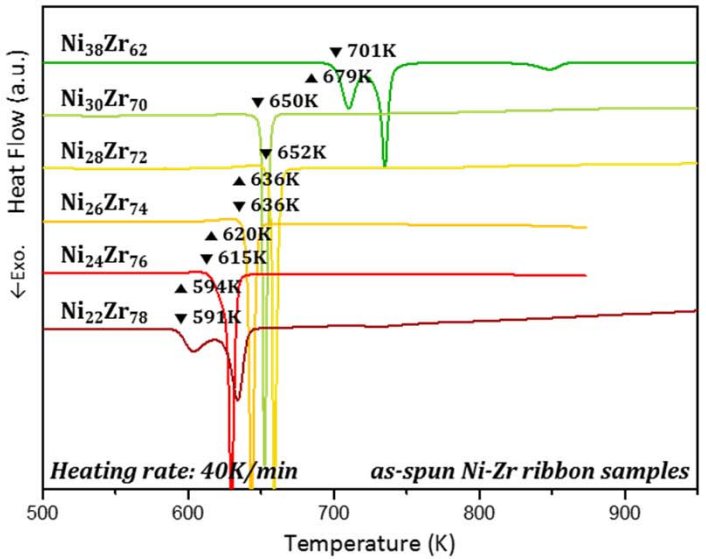

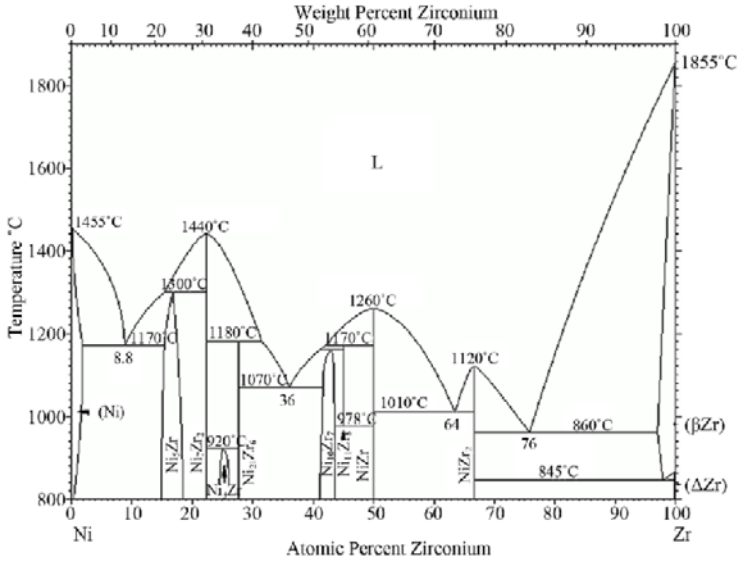

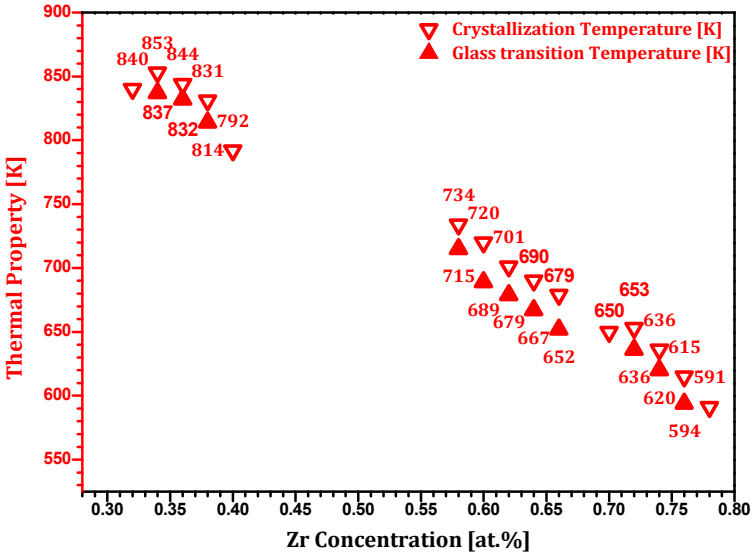

Zr content	$Ni_{68}Zr_{32}$	$Ni_{66}Zr_{34}$	$Ni_{64}Zr_{36}$	$Ni_{62}Zr_{38}$	$Ni_{60}Zr_{40}$	$Ni_{42}Zr_{58}$	$Ni_{40}Zr_{60}$	$Ni_{38}Zr_{62}$	$Ni_{36}Zr_{64}$	$Ni_{34}Zr_{66}$	$Ni_{30}Zr_{70}$	$Ni_{28}Zr_{72}$	$Ni_{26}Zr_{74}$	$Ni_{24}Zr_{76}$	$Ni_{22}Zr_{78}$
T_g [K]		837	832	814		715	689	679	667	652		636	620	594	
T_x [K]	840	853	844	831	792	734	720	701	690	679	650	653	636	615	591

5.5. Thermal Stability of Metallic Glasses

(b) Arrhenius plot of the incubation time for the precipitation of crystalline phases (τ) in the $Zr_{65}Al_xCu_{35-x}$ (x=0, 7.5, 20) alloys

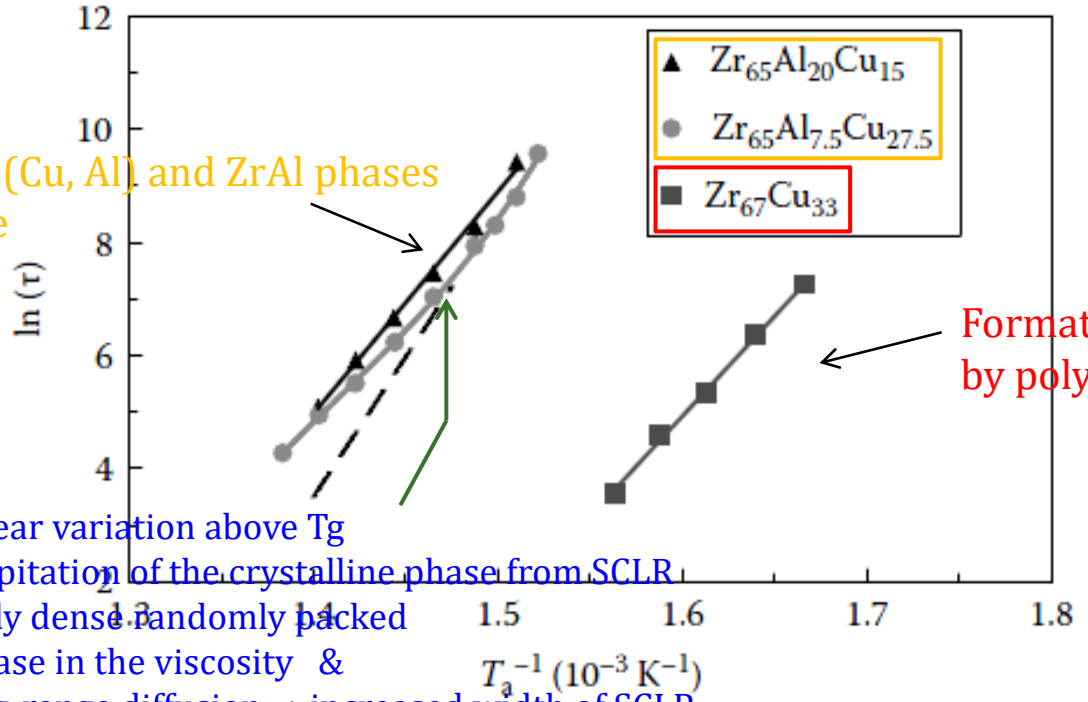

$$\tau \propto \frac{T\eta}{(T_\ell - T)^2}$$

Formation of $Zr_2(Cu, Al)$ and ZrAl phases by eutectic mode

Formation of Zr_2Cu phase by polymorphous mode

Shifted from the linear variation above Tg → suppressed precipitation of the crystalline phase from SCLR due to possess highly dense randomly packed structures → increase in the viscosity & difficult to have long-range diffusion → increased width of SCLR

FIGURE 5.8
Arrhenius plot of the incubation time, τ for the precipitation of crystalline phases in the binary $Zr_{67}Cu_{33}$, and ternary $Zr_{65}Al_{7.5}Cu_{27.5}$ and $Zr_{65}Al_{20}Cu_{15}$ alloys. Note the deviation of τ to the positive side of the linear variation (to higher temperatures) only for the ternary $Zr_{65}Al_{7.5}Cu_{27.5}$ alloy, signifying the delayed crystallization in the alloy with 7.5 at.% Al. Such a deviation is not observed for the other alloys. (Reprinted from Inoue, A. et al., *Mater. Sci. Eng. A*, 178, 255, 1994. With permission.)

(C) Annealing up to T_a at a heating rate of 0.17 K/s (10K/min), annealed there for 60s
→ measure peak temperatures for the nucleation and growth reactions of the crystalline phases in the $Zr_{65}Al_xCu_{35-x}$ (x=0, 7.5) alloys

* Difference in the reciprocals of the Tp between the Pre-annealed and as-quenched samples

688 K, correspond to the peak temp. of the nucleation event of a crystalline phase formation

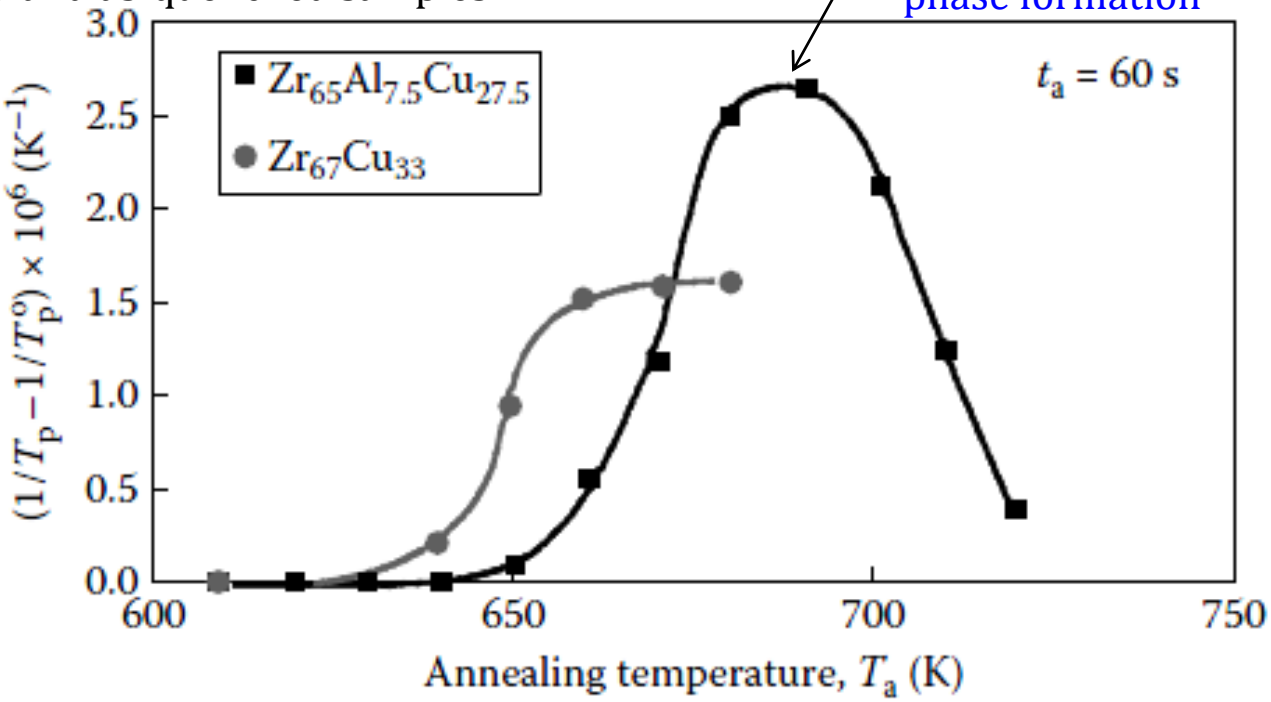

* Measure Tx at a very high heating rate of 5.33 K/s (320 K/min) = corresponding to the maximum growth rates, that is growth temperature
  - Zr67Cu33: Just above the maximum temp of 670 K/ difference ~ very small
  - Zr65Al7.5Cu27.5: the difference btw max nucleation and max growth temp. ~143K, resulting in enhanced resistance to crystallization (high thermal stability)
* Heating rate ↑ – not significantly increase the grain size in Zr67Cu33 ↔ considerably large grain size in Zr65Al7.5Cu27.5 due to the presence of fewer nuclei

5.7. Annealing of Bulk Metallic Glasses: SR → SCLR (& PS) → Crystallization

Figure 5.11 Different pathways for a metallic glass to crystallize into the equilibrium phases

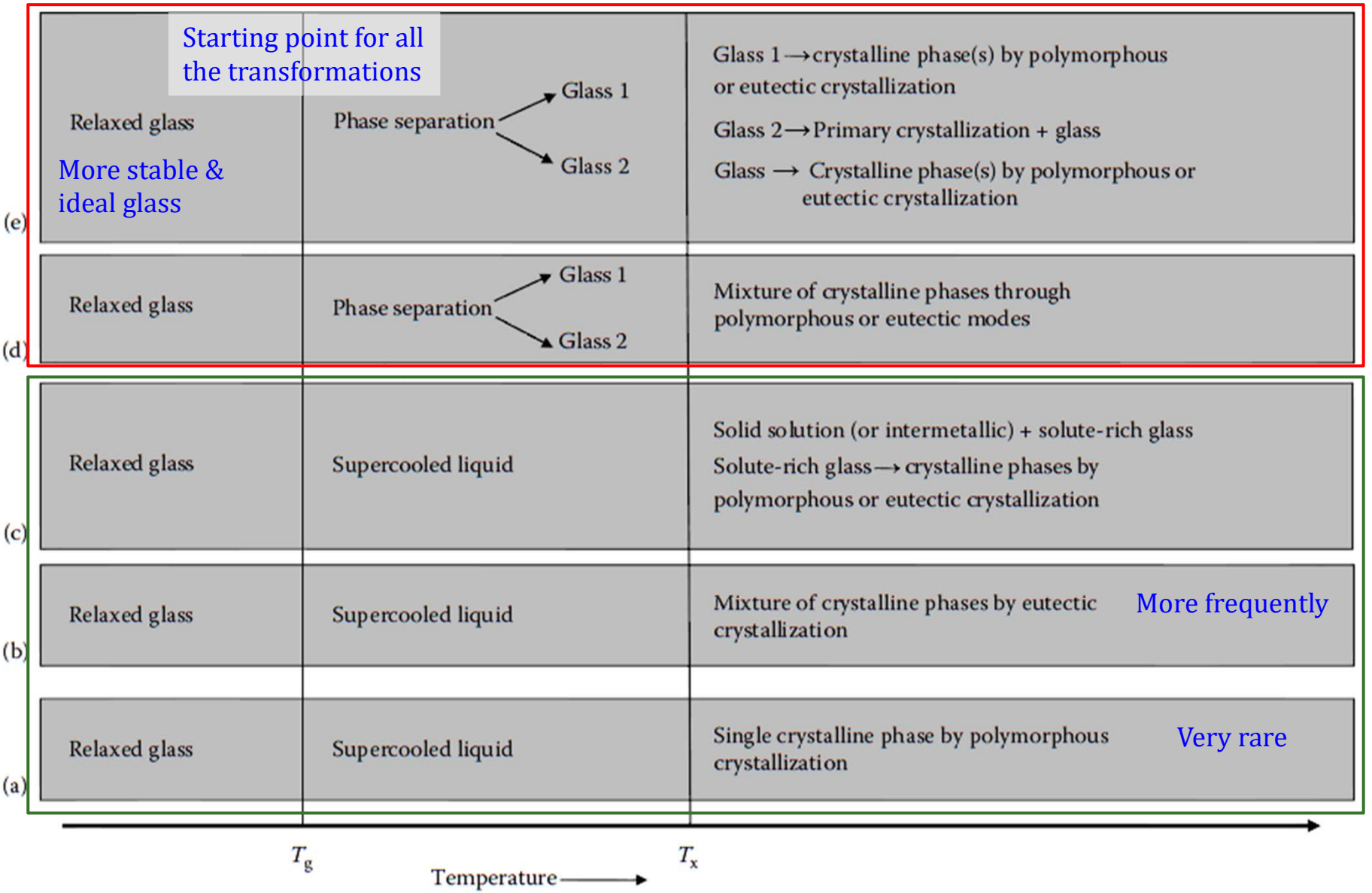

5.7. Annealing of Bulk Metallic Glasses: SR → SCLR (& PS) → Crystallization

5.7.1 Structural Relaxation

RELAXATION BEHAVIOR

Structural relaxation = stabilization

On annealing, the as-synthesized glass slowly transforms toward an "ideal" glass of lower energy through structural relaxation. = annihilation of "defects" or free volume, or recombination of the defects of opposing character, or by changes in both topological and compositional SRO

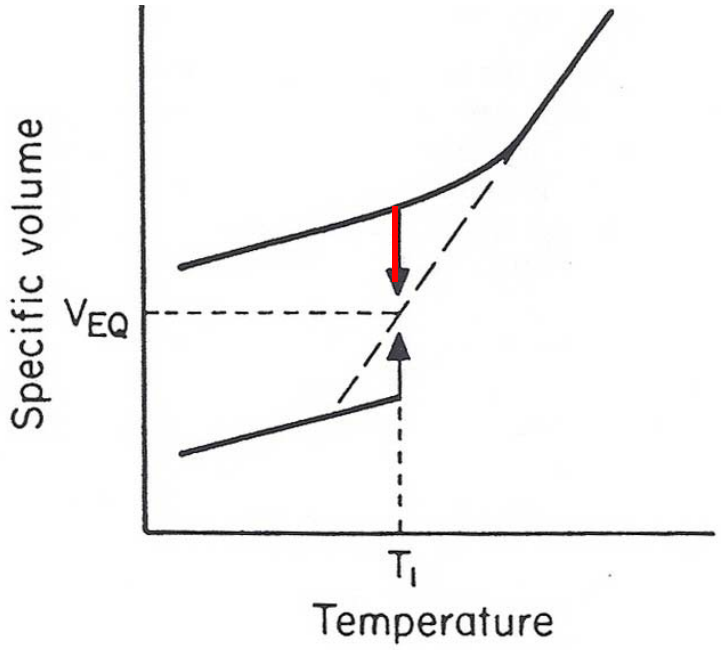

Fig. 9a. Relaxation from initial volumes above and below the equilibrium volume (schematic)

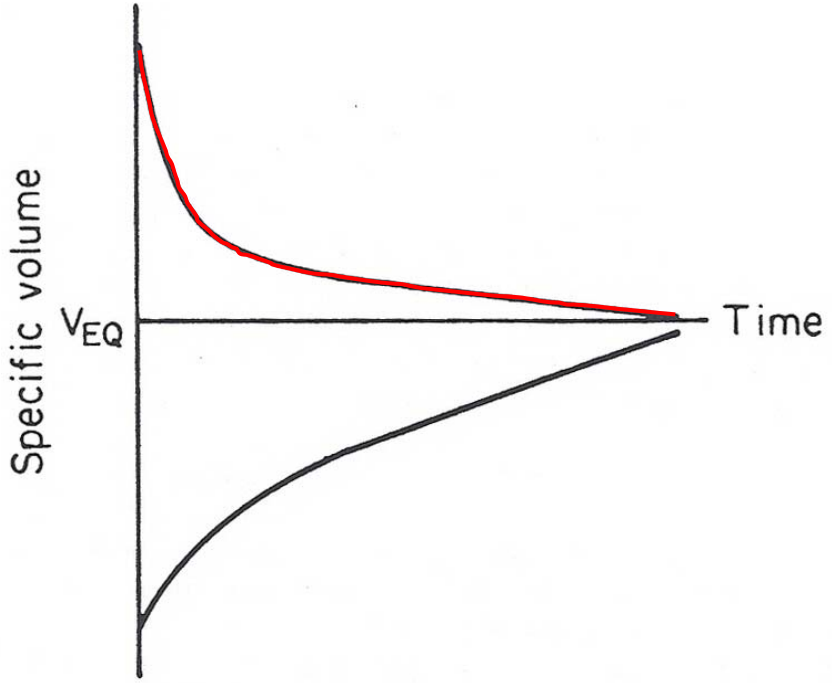

Fig. 9b. Variation of volume with time for initial volumes above and below the equilibrium volume (schematic)

5.7.1 Structural Relaxation

CSRO: Chemical short-range order ⟺ TSRO: Topological short-range order

* Relaxation process

(a) Low temp. regimes (sub-sub-Tg, i.e., Tg-200K <Ta<Tg-100K)

(b) High temp. regimes (sub-Tg, i.e., Ta ≥ Tg-100K)

Exception: Pd-Si, Fe-B and Zr-Cu : undergo structural relaxation just above RT

* Structural relaxation in metallic glasses by a low temperature annealing process

→ does not cause crystallization but significant changes in physical properties

* Relaxed glass : decreased specific heat, reduced diffusivity, reduced magnetic anisotropy, increased elastic constants (by about 7%), significantly increased viscosity (by more than 5 orders of magnitude) and loss of (bend) ductility in some glasses, in addition to changes in elastic resistivity (by about 2 %), Curie temperature (by as much as 40 K), enthalpy (by about 200-300 cal/mol), superconductivity, and several other structure-sensitive properties.

& Density changes: a small increase in density (about 0.5% for melt-spun ribbons and a smaller value of about 0.1%-0.15% for BMG alloys)

5.7.1 Structural Relaxation

* Density changes: a small increase in density (about 0.5% for melt-spun ribbons and a smaller value of about 0.1%-0.15% for BMG alloys)

TABLE 5.3

Changes in the Bulk Densities, ρ (g cm^{-3}) of Metallic Glassy Alloys in the As-Solidified and Structurally Relaxed Conditions

Alloy Composition	Synthesis Method	Rod Diameter (mm)/Ribbon Thickness	$\rho_{as\text{-}solidified}$	$\rho_{relaxed}$	$\Delta\rho_{relaxed}$ (%)	Reference
$Pd_{77.5}Cu_6Si_{16.5}$	Melt spinning	30 μm thick ribbon	10.46	10.51	0.48	[68]
$Pd_{40}Cu_{30}Ni_{10}P_{20}$	Melt spinning	40 μm thick ribbon	9.318	9.337	0.2	[69]
$Pd_{77.5}Cu_6Si_{16.5}$	Water quenching	2 mm dia rod	10.48	10.51	0.29	[68]
$Pd_{40}Cu_{30}Ni_{10}P_{20}$	Cu-mold casting	5 mm dia rod	9.27	9.28	0.11	[70]
$Zr_{55}Cu_{30}Al_{10}Ni_5$	Cu-mold casting	5 mm dia rod	6.82	6.83	0.15	[70]

Note: $$\Delta\rho_{relaxed} = \frac{\rho_{relaxed} - \rho_{as\text{-}solidified}}{\rho_{as\text{-}solidified}}.$$

* Measurement of structural relaxation in metallic glasses:

- Electrical resistivity measurements (CSRO < TSRO) and DSC (most popular technique)
- Mossbauer spectroscopy (determine the atomic environments)
- Hardness measurement (increased)
- Diffraction techniques (X-ray, neutron, and electron scattering methods)

(sharpening of the PDF peaks, without shifting their position)

→ The first stage of relaxation was suggested to be related to the elimination of short and long inter-atomic distances and the second stage to the local chemical reordering in the glassy phase (phase separation and nano-crystallization after annealing at higher temp.

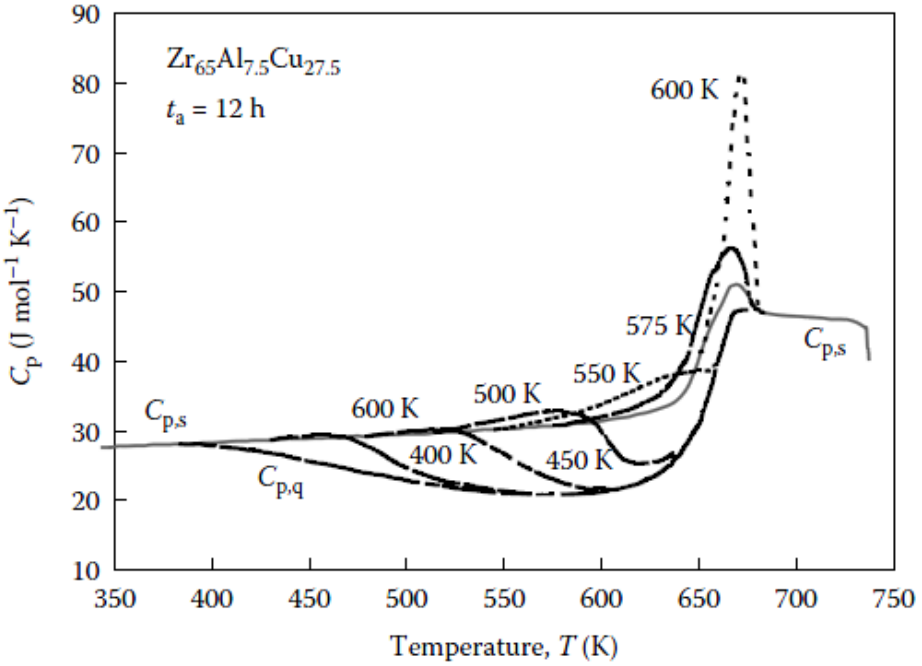

FIGURE 5.12
The variation of specific heat, C_p with annealing temperature, T_a for a glassy $Zr_{65}Al_{7.5}Cu_{27.5}$BMG alloy annealed for 12 h at different temperatures from 400 to 620 K. The solid line represents the variation of C_p for the reference sample annealed for 12 h at 690 K. (Reprinted from Inoue, A. et al., *J. Non-Cryst. Solids*, 150, 396, 1992. With permission.)

→ dependent on thermal history, excess endothermic peak (recoverable), exothermic broad peak (irrecoverable)

With increasing T_a, the maximum in $\Delta C_{p,endo}$ for the two alloys initially increases gradually, followed by a rapid increase at temperatures just below T_g, and then a rapid decrease above T_g.

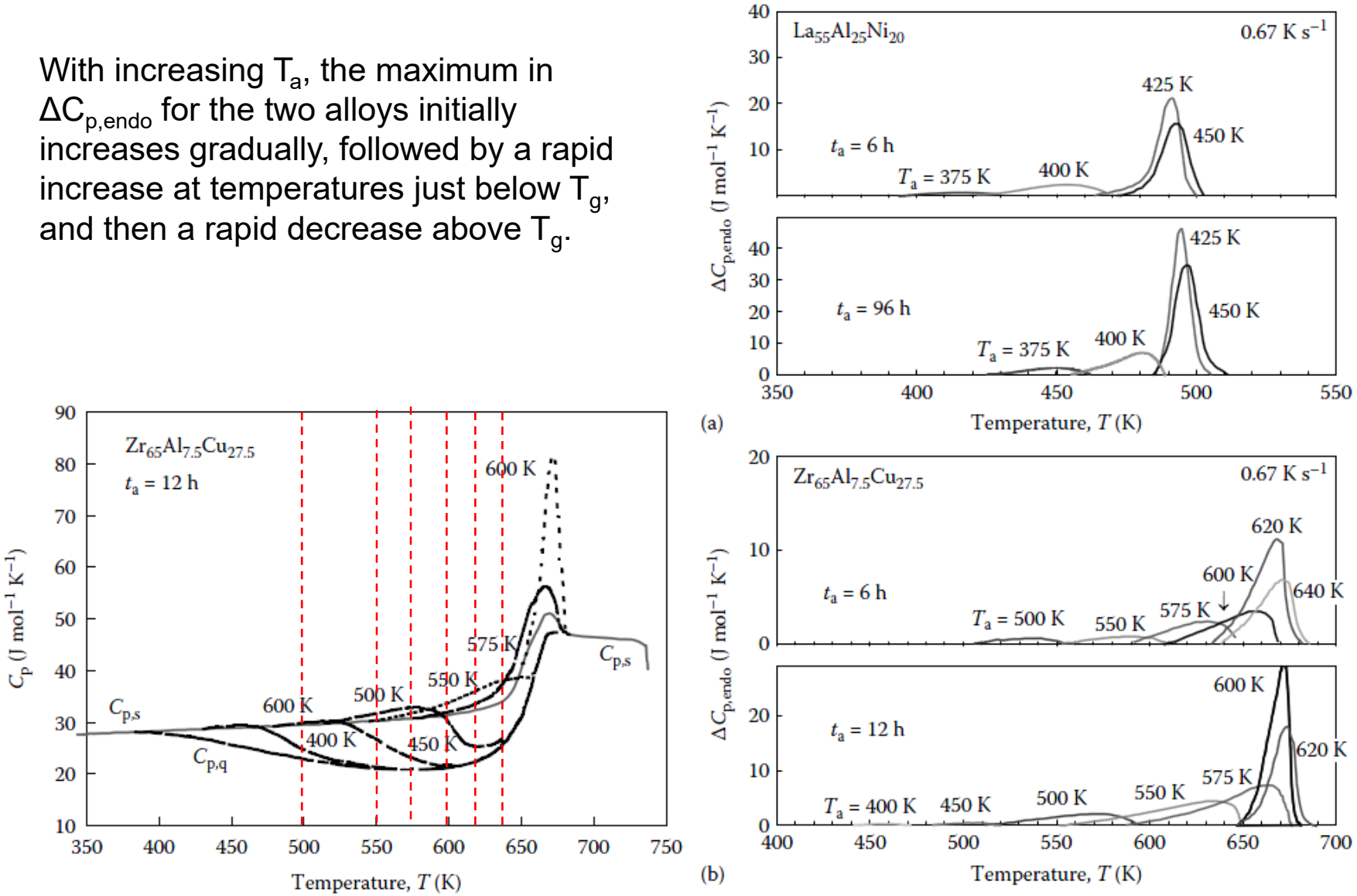

FIGURE 5.13
The differential specific heat, $\Delta C_p(T)$, between the reference and annealed samples for the glassy (a) $La_{55}Al_{25}Ni_{20}$ and (b) $Zr_{65}Al_{7.5}Cu_{27.5}$ alloys annealed for 6 and 96 h for the $La_{55}Al_{25}Ni_{20}$ alloy and for 1 and 12 h in the case of $Zr_{65}Al_{7.5}Cu_{27.5}$ alloy at different temperatures. The samples have been heated in a DSC at 0.67 K s^{-1} (40 K min^{-1}). (Reprinted from Inoue, A. et al., *J. Non-Cryst. Solids*, 150, 396, 1992. With permission.)

* Assuming that the change in enthalpy is entirely due to structural changes in the glassy state and that the average free volume per atom (=V_f/V_m, where V_f is the free volume and V_m is the atomic volume) is proportional to the change in enthalpy:

$$\frac{V_f}{V_m} = C\Delta H \tag{5.5}$$

where C is a constant. The proportionality constant C is determined by first calculating V_f using the Grest and Cohen model [83]:

$$V_f = \frac{k}{2s_0}\left(T - T_0 + \sqrt{(T-T_0)^2 + \frac{4V_a s_0}{k}T}\right) \tag{5.6}$$

$Zr_{44}Ti_{11}Ni_{10}Cu_{10}Be_{25}$ glassy

where k is the Boltzmann constant. The appropriate fit parameters for the above alloy were reported to be: $bV_m s_0/k = 4933\,\text{K}$ with $b = 0.105$, $4V_a s_0/k = 162\,\text{K}$, $T_0 = 672\,\text{K}$. V_m for this alloy has been reported to be 1.67×10^{-29} m^3 near the liquidus temperature. Thus, by calculating V_f from Equation 5.6, V_f/V_m can be calculated.

→ The mechanical properties of metallic glasses (including the BMGs) are affected by the magnitude of free volume present in them. Hence, it becomes important to be able to quantitatively determine the free volume present in the glass to relate the magnitude of free volume to the changes in mechanical properties.

Anelasticity in metallic glass

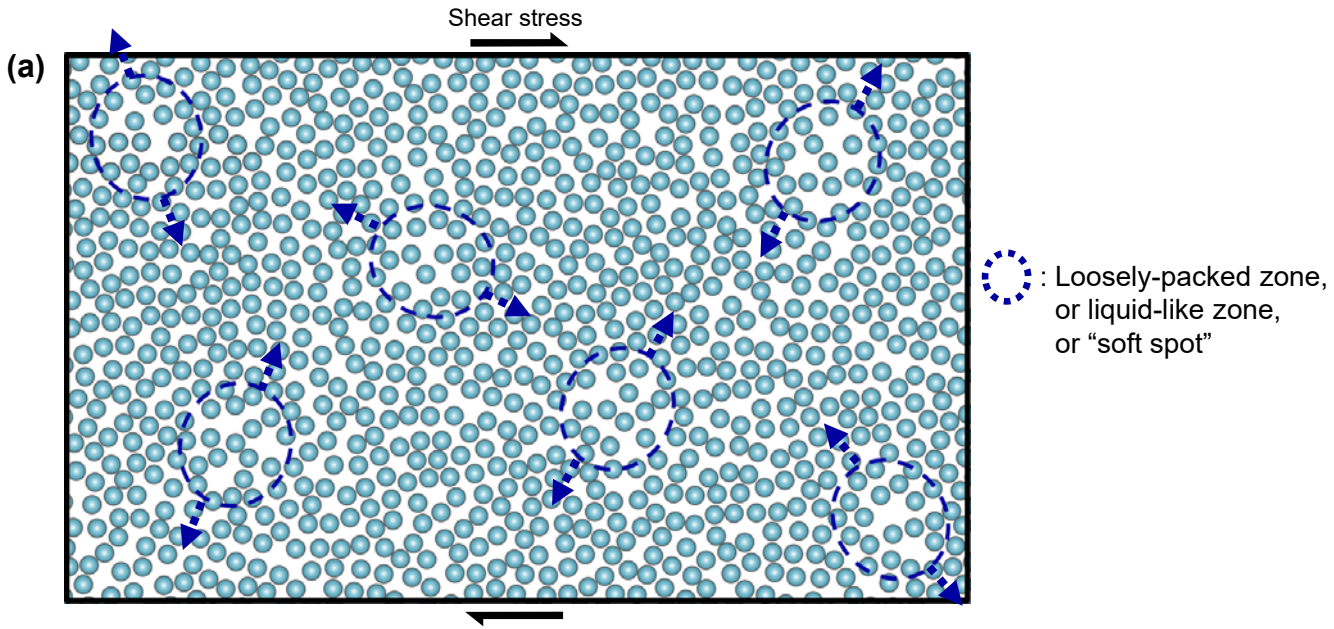

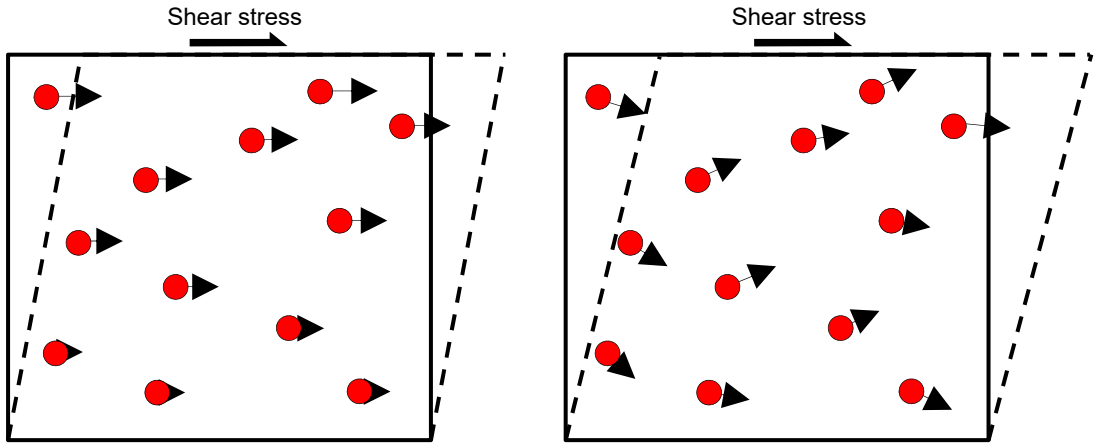

(b) Quasi continuum

(c) Actual displacement in metallic glass

Weaire et al., *Acta Metall.* **1971,** *19*, 779-788.

DMA measurement : Phase lag, storage modulus and loss modulus

Perfectly elastic (time-independant)

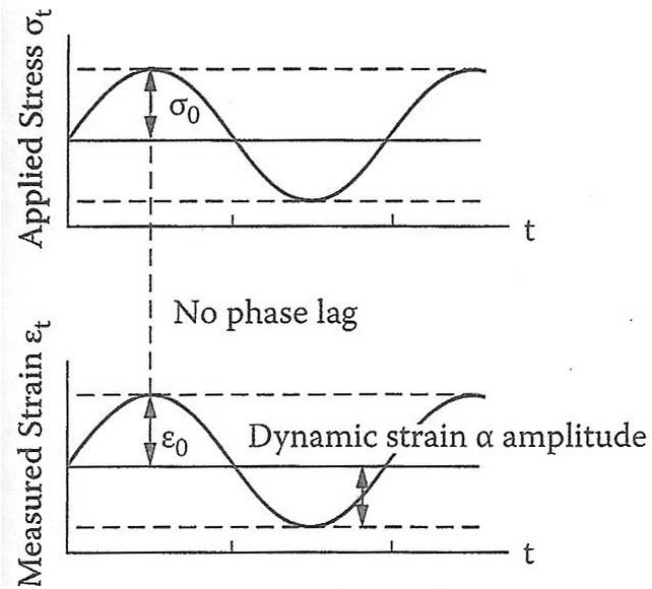

Anelastic (Viscoelastic, time-dependant)

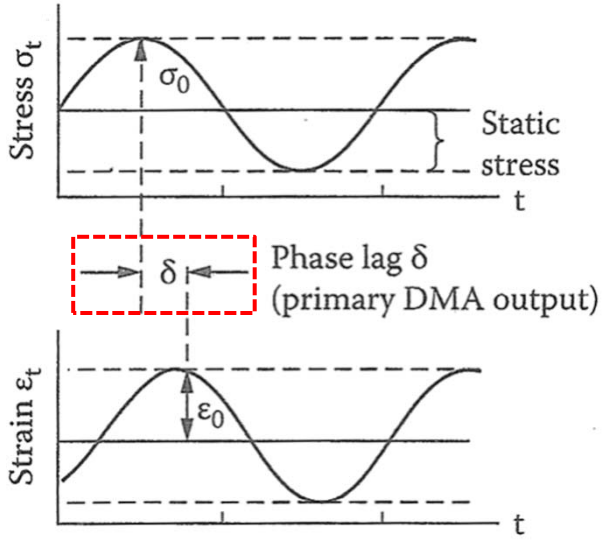

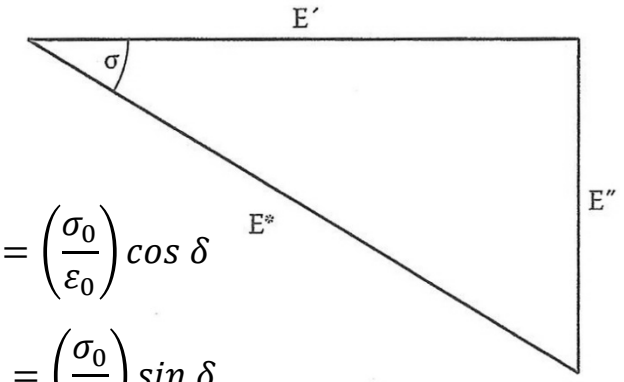

$$E' = \left(\frac{\sigma_0}{\varepsilon_0}\right) cos\ \delta$$

$$E'' = \left(\frac{\sigma_0}{\varepsilon_0}\right) sin\ \delta$$

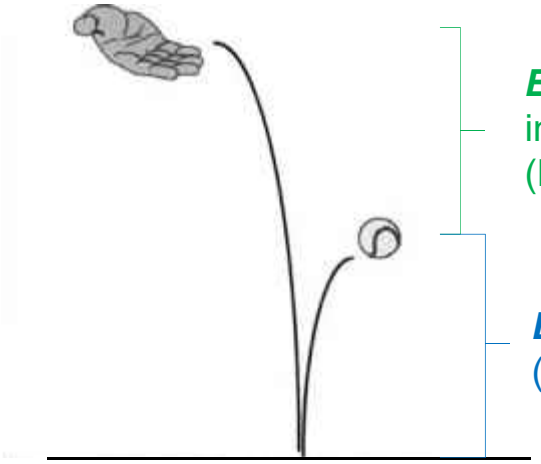

E" : Energy loss in internal motion (loss modulus)

E' : Elastic response (storage modulus)

Menard, K. P., *Dynamic Mechanical Analysis: A Practical Introduction, Second Edition*. CRC Press: 2008.

α- and β- relaxations of glass-forming liquids

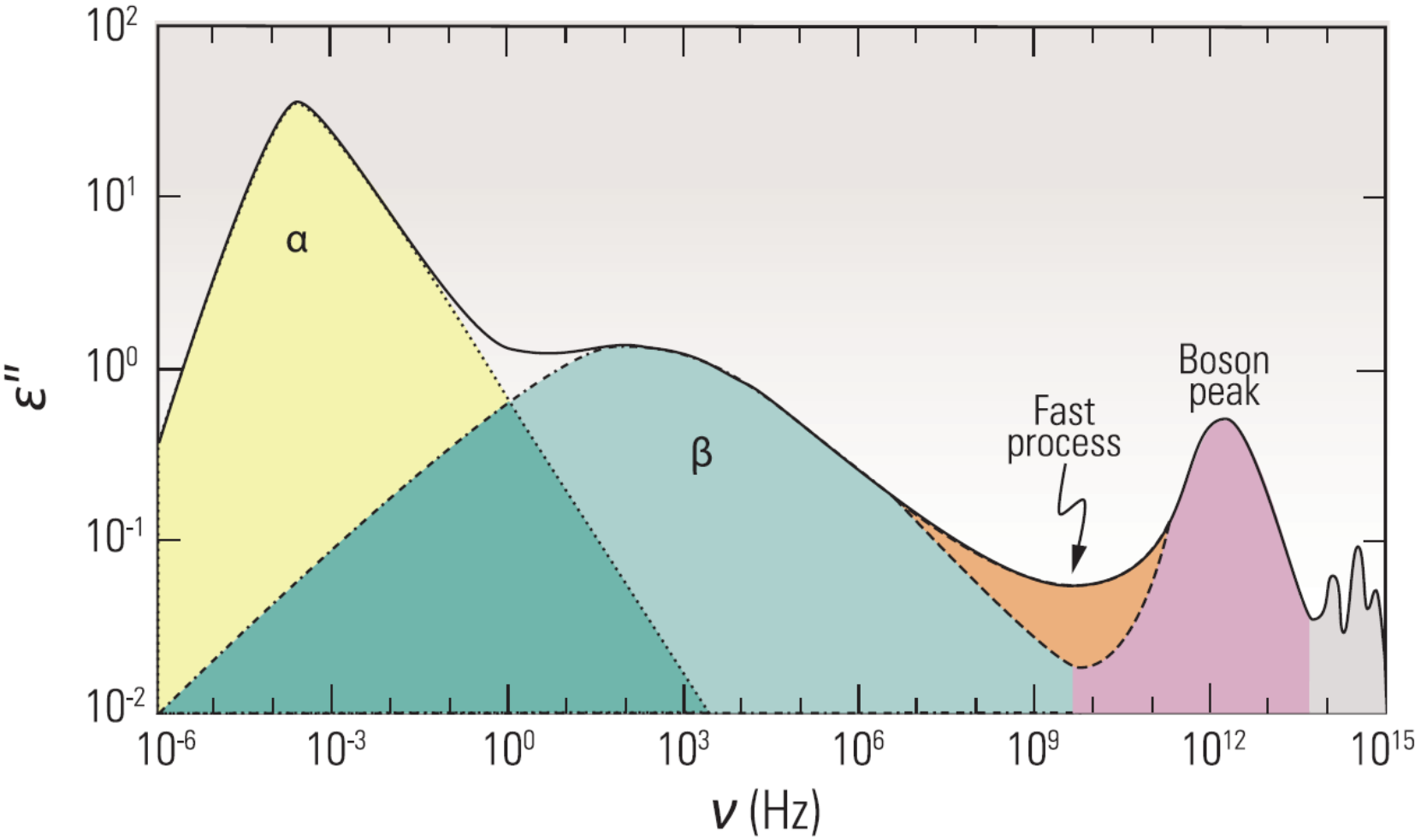

Schematic dielectric spectrum of relaxation dynamics of glass-forming liquids

Yu, H. B., et al. (2014). "The β-relaxation in metallic glasses." *National Science Review* **1**(3): 429-461.

Decoupling of translational & rotational diffusion in supercooled liquid

* glass-forming mixture chlorobenzene/cis-decalin

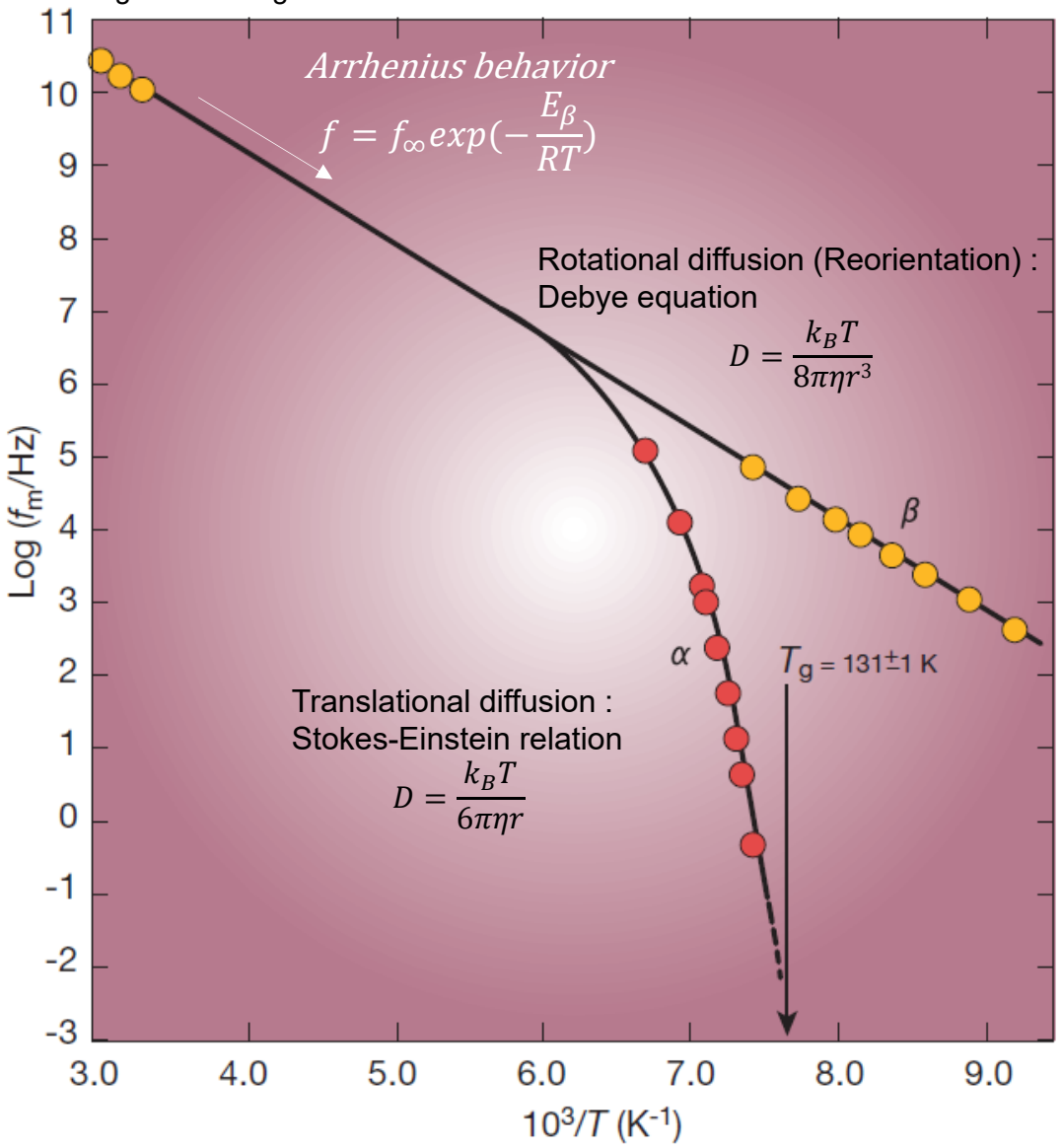

Debenedetti, P. G. and F. H. Stillinger (2001). "Supercooled liquids and the glass transition." *Nature* **410**(6825): 259-267.

Temperature dependence of relaxation time
: α relaxation (VFT) & β relaxation (Arrhenius)

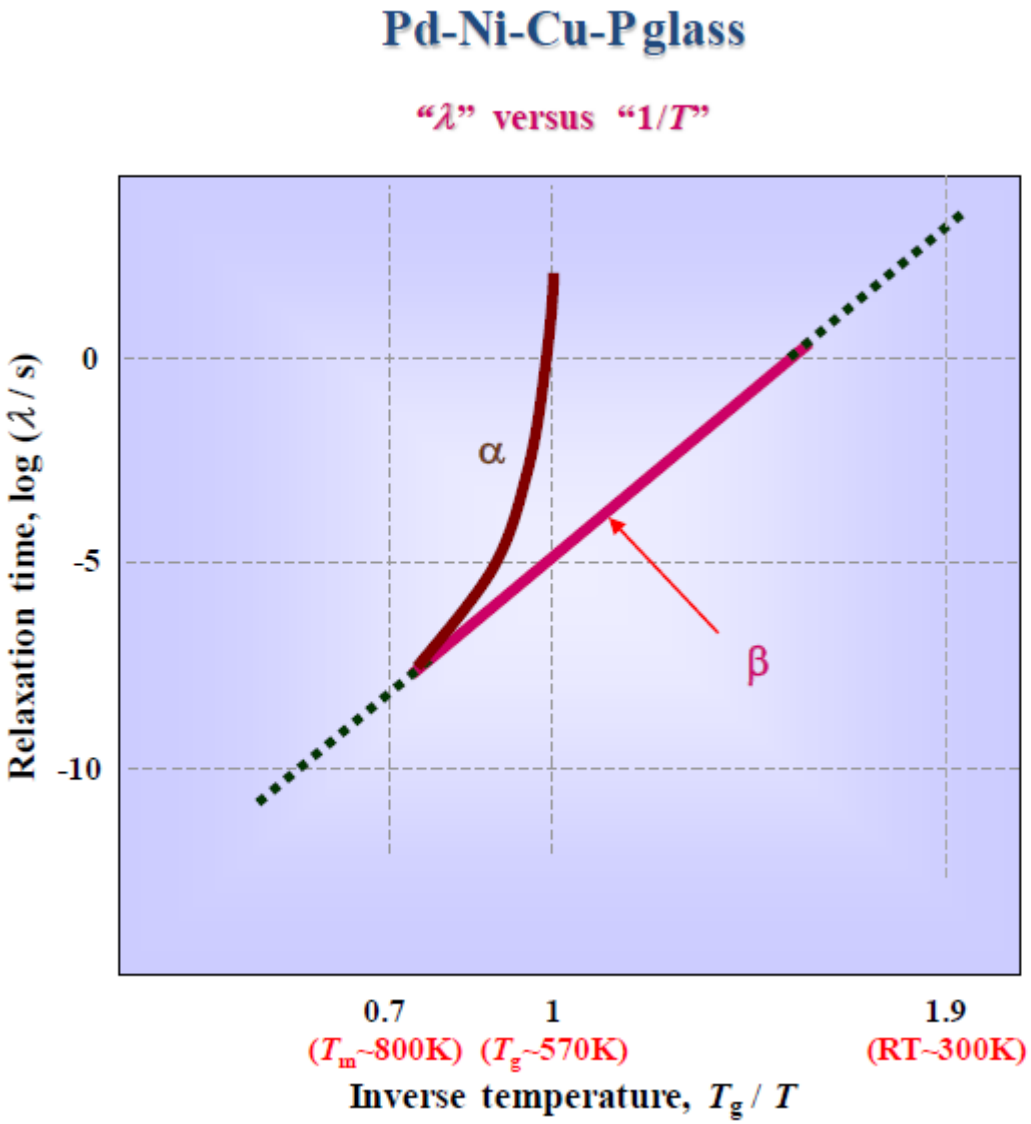

α VFT

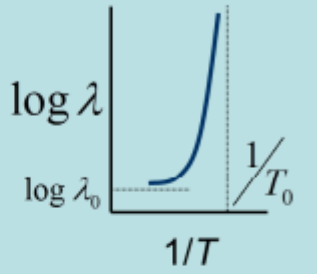

$$\lambda_\alpha = \lambda_{\alpha 0} \exp\left(\frac{Q_\alpha}{T - T_0}\right)$$

Arrhenius β

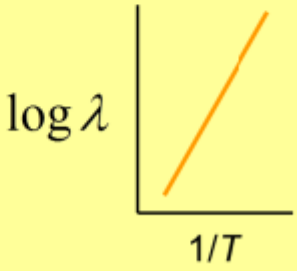

$$\lambda_\beta = \lambda_{\beta,0} \exp\left(\frac{Q_\beta}{kT}\right)$$

Potential Energy landscape of supercooled liquids and glass formation

Potential energy function $\boldsymbol{\Phi}(\boldsymbol{r_1}, \boldsymbol{r_2}, \cdots, \boldsymbol{r_N})$

(where $\boldsymbol{r_i}$ is spatial location for each of particles in a system),

including every chemical characteristics in the system.

- Coordinates of N particles → *3N + α'* dimensional space

- Number of minima $\Omega(N) \sim N! \exp(\alpha N)$

  : Drastically increased with *N*

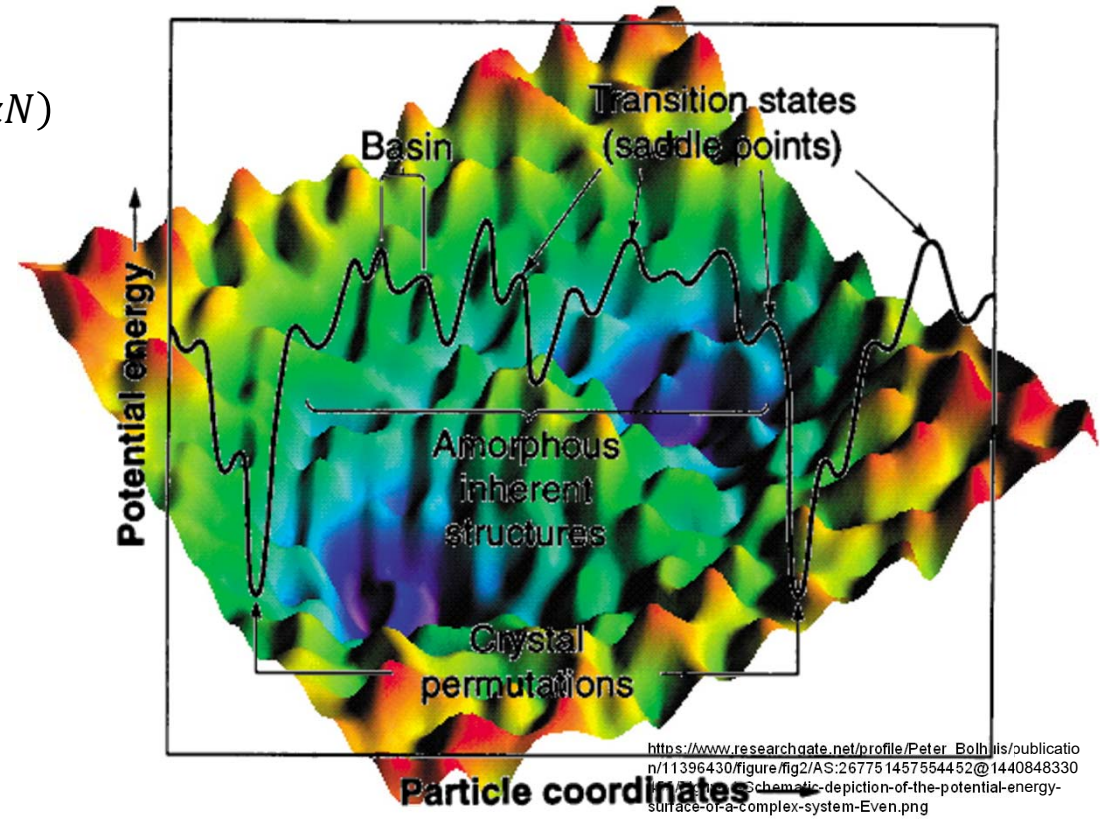

https://www.researchgate.net/profile/Peter_Bolhuis/publication/11396430/figure/fig2/AS:267751457554452@1440848330[illegible]Schematic-depiction-of-the-potential-energy-surface-of-a-complex-system-Even.png

Stillinger, F. H. (1995). "A Topographic View of Supercooled Liquids and Glass Formation." *Science* **267**(5206): 1935-1939.

Potential Energy landscape of supercooled liquids and glass formation

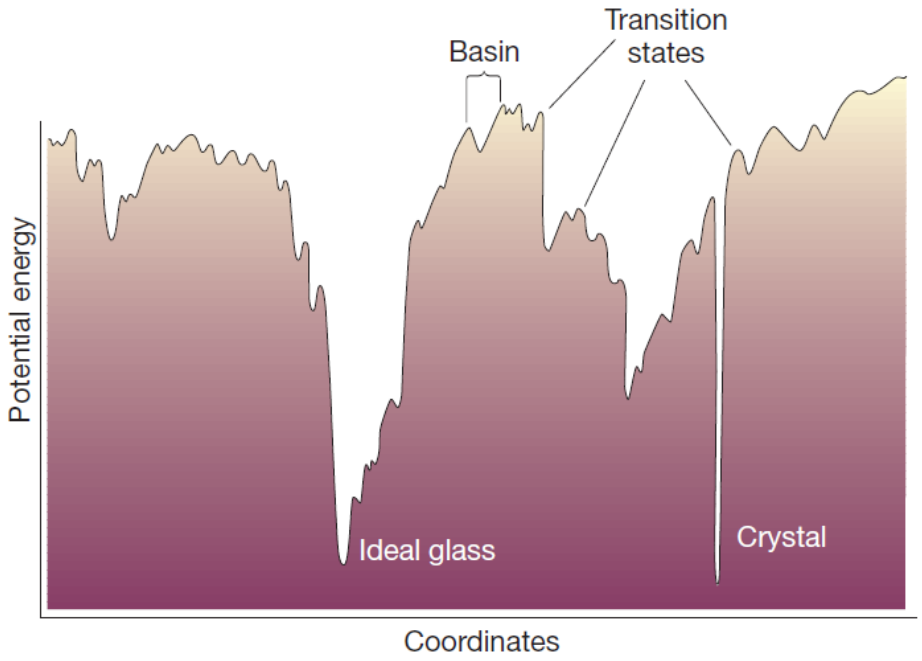

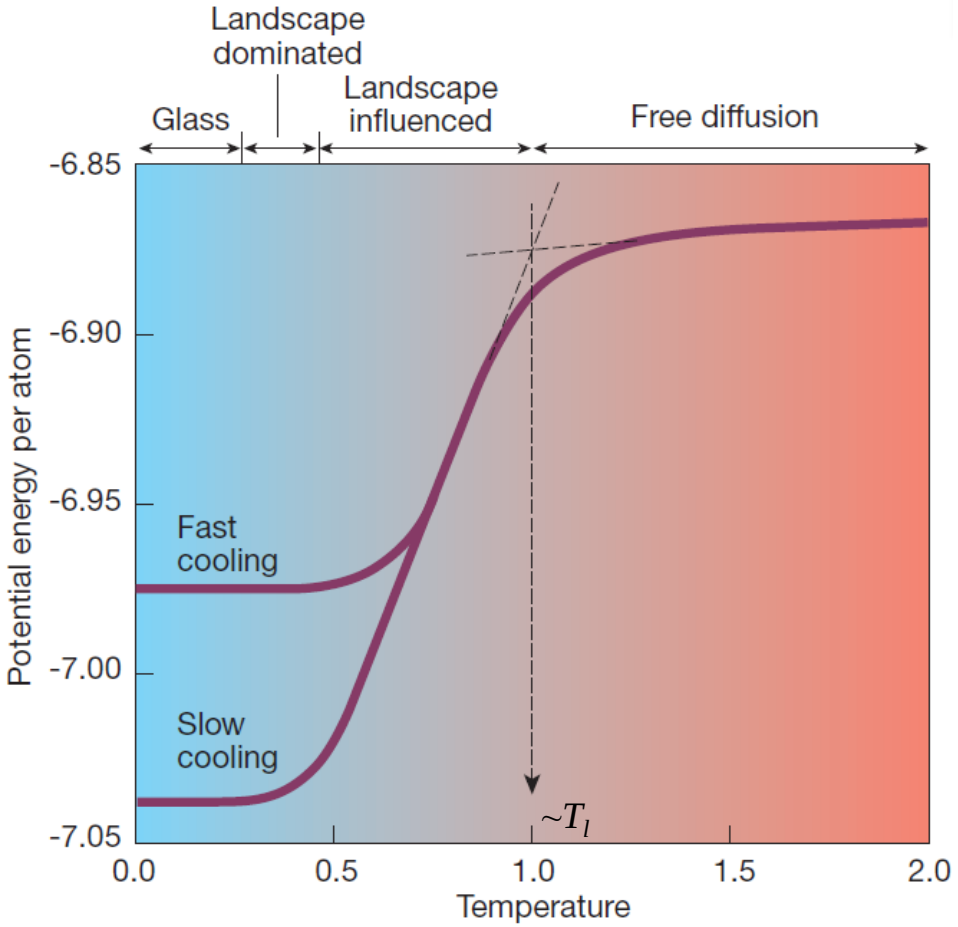

Debenedetti, P. G. and F. H. Stillinger (2001). "Supercooled liquids and the glass transition." *Nature* **410**(6825): 259-267.

Dynamic mechanical relaxations in typical glasses

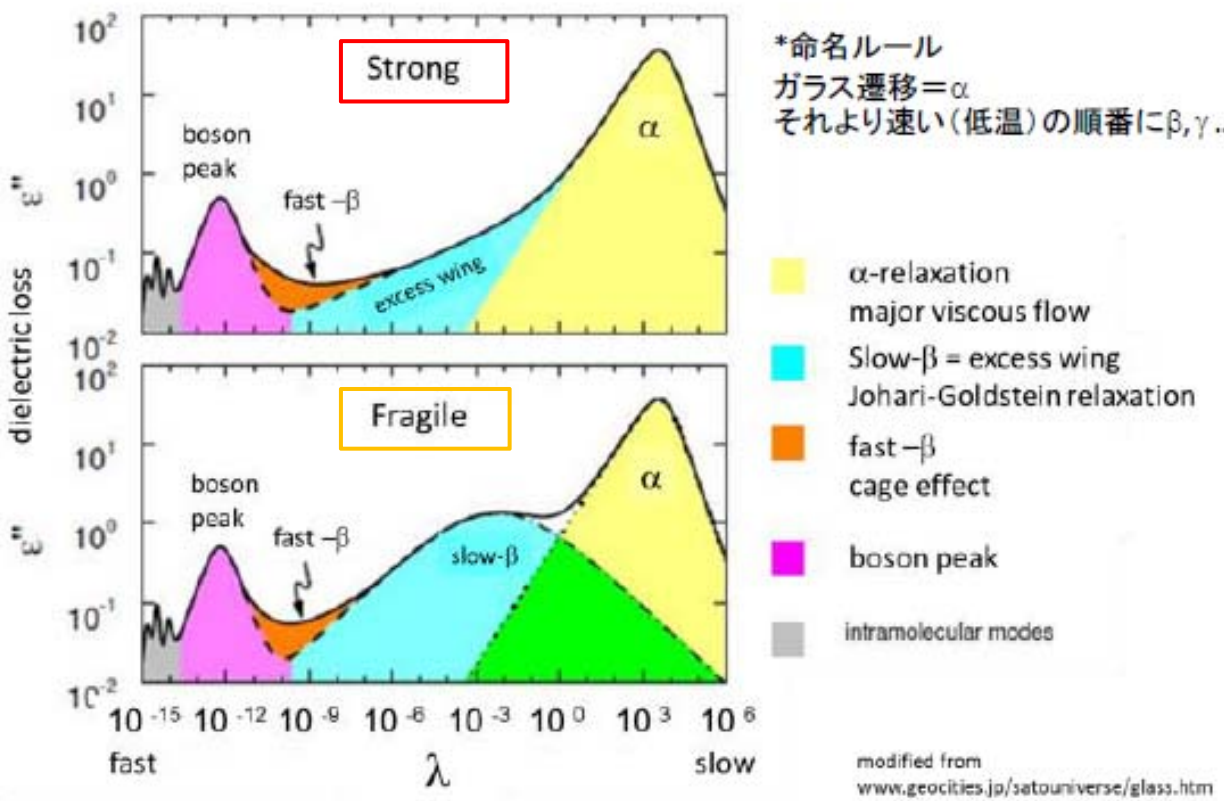

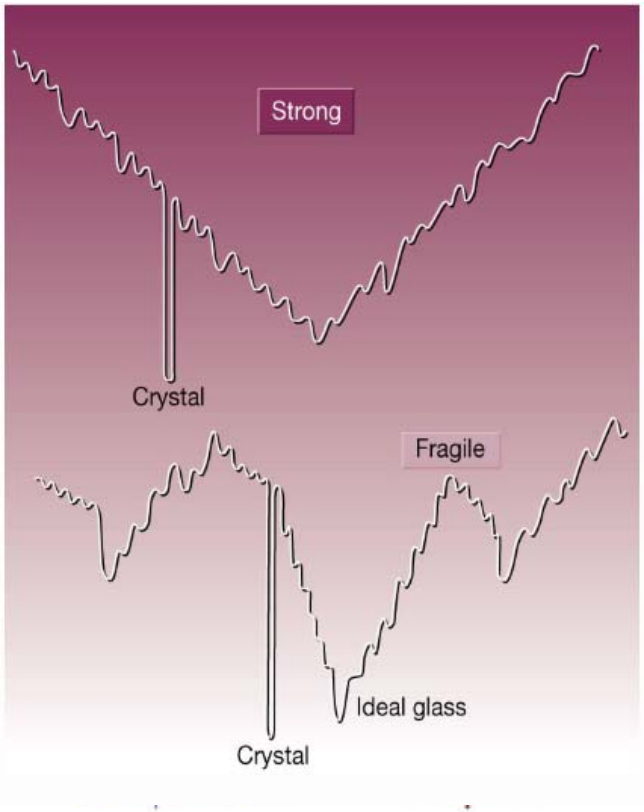

Strong: small deviation of activation E
between α relaxation and β relaxation

Fragile: large deviation of activation E
between α relaxation and β relaxation

Schematic representation of the energy landscapes of strong and fragile substances.

First report on an "excess wing" in metallic glass

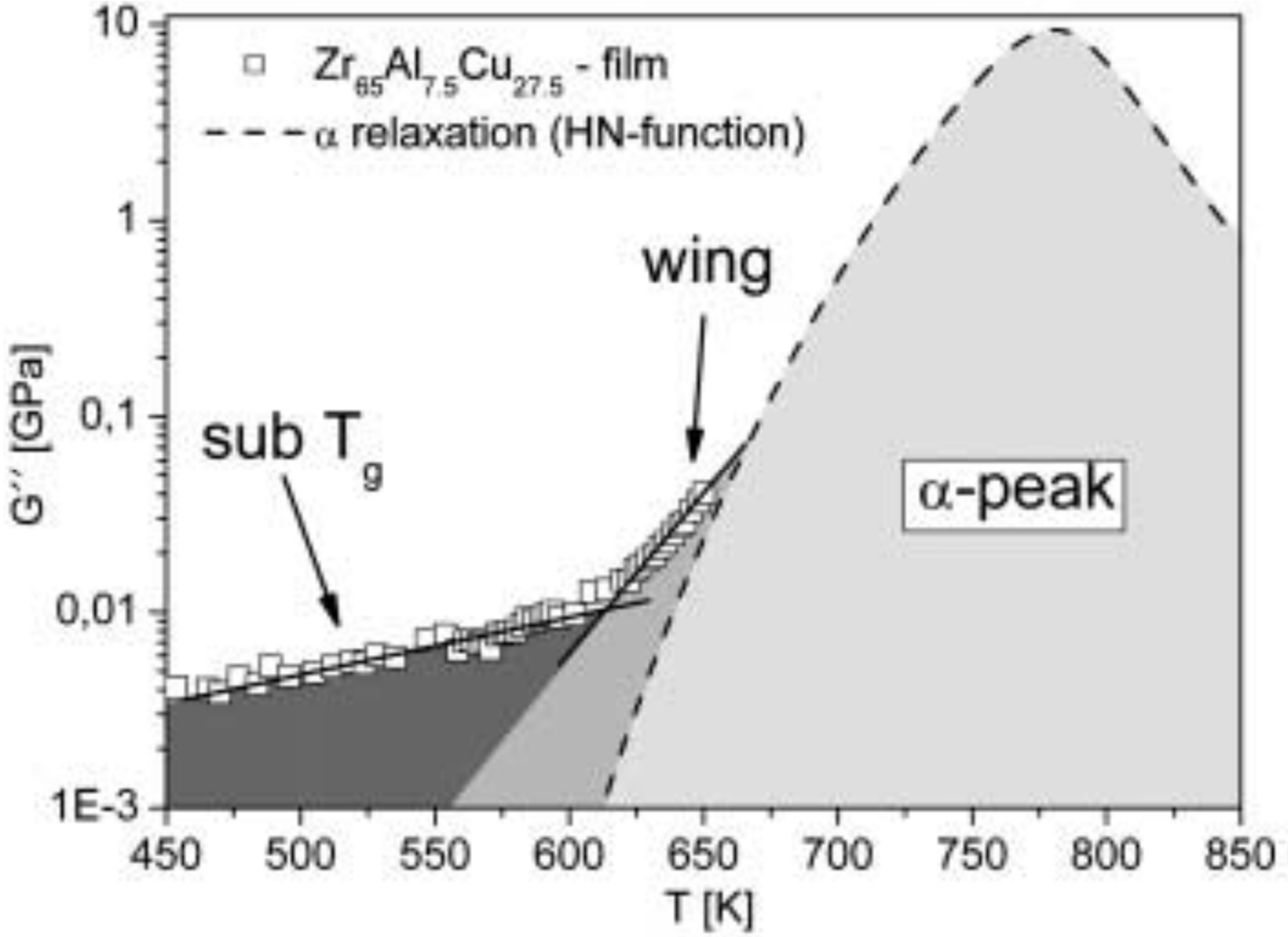

Rösner et al., Indications for an "excess wing" in metallic glasses from the mechanical loss modulus in $Zr_{65}Al_{7.5}Cu_{27.5}$. *Europhysics Letters* **68,** 226 (2004).

Alpha- & Beta-relaxation in metallic glasses

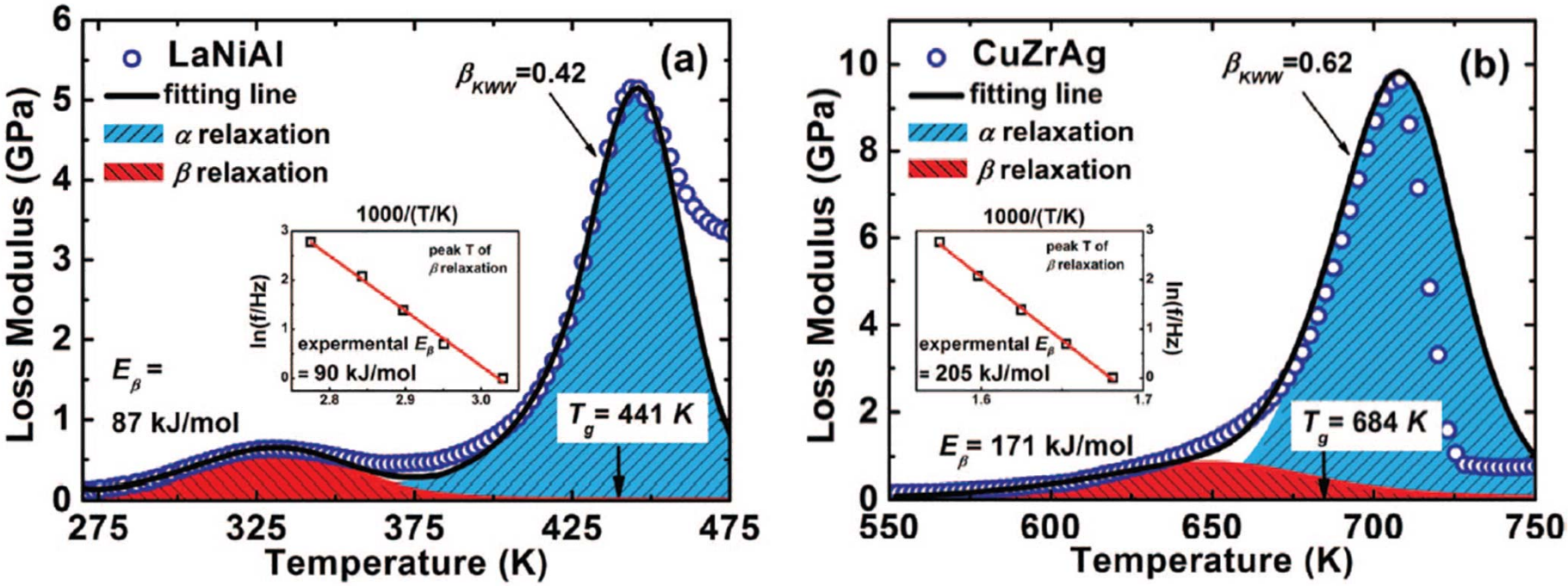

Ngai et al., *The Journal of Chemical Physics* **2013,** *139*, 014502.

Relaxations of metallic glass

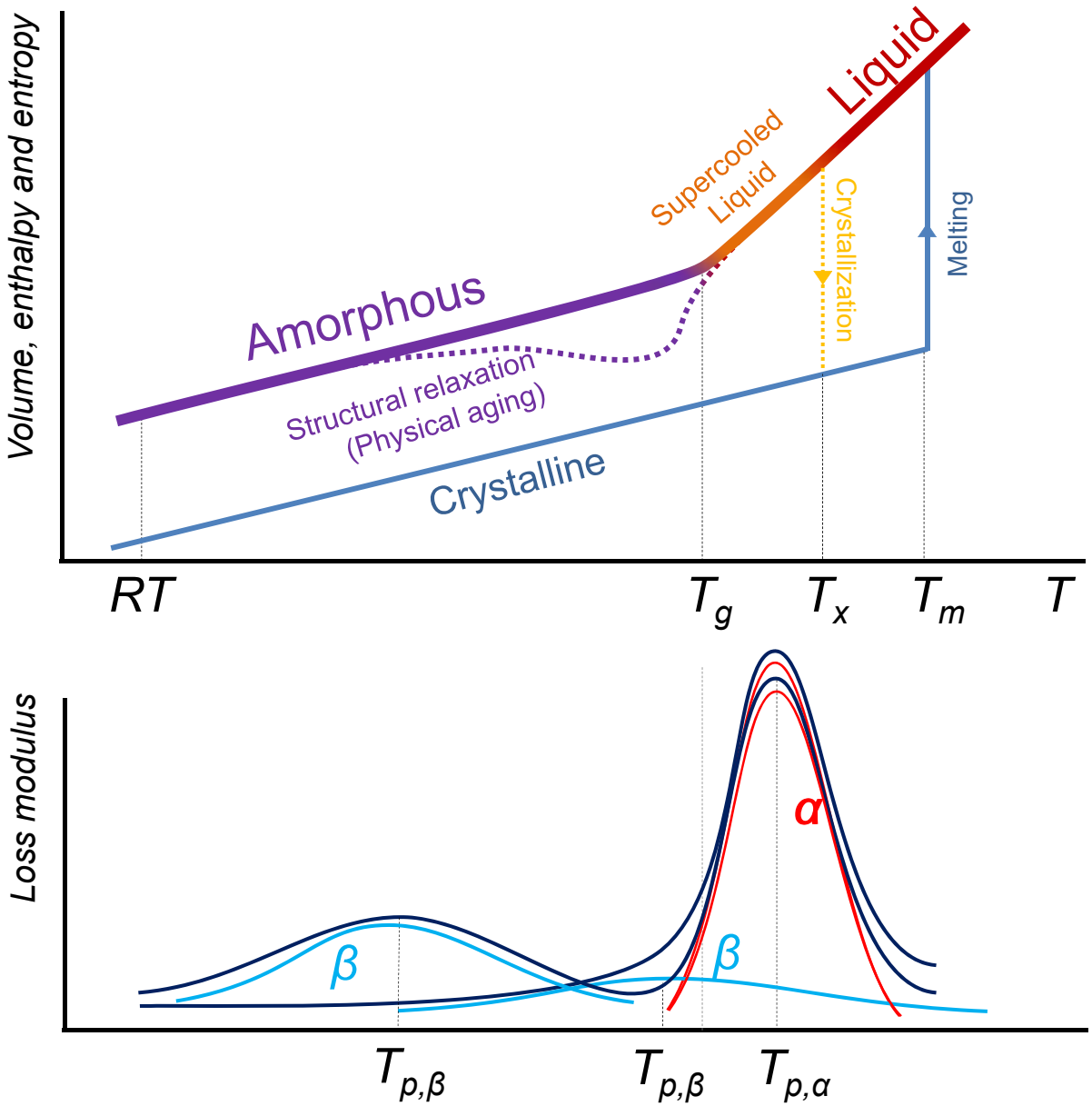

- Structural relaxation (Physical aging)
  - Irreversible
  - Decrease of free volume
  - Enthalpy and entropy change toward equilibrium state
- α-relaxation (Primary)
  - Irreversible
  - Dominant at over T_g
  - Primarily related to glass transition
- β-relaxation (Secondary)
  - Reversible
  - Initiate at high T and continue below T_g

Relaxation spectrum depending on alloy system and compositions

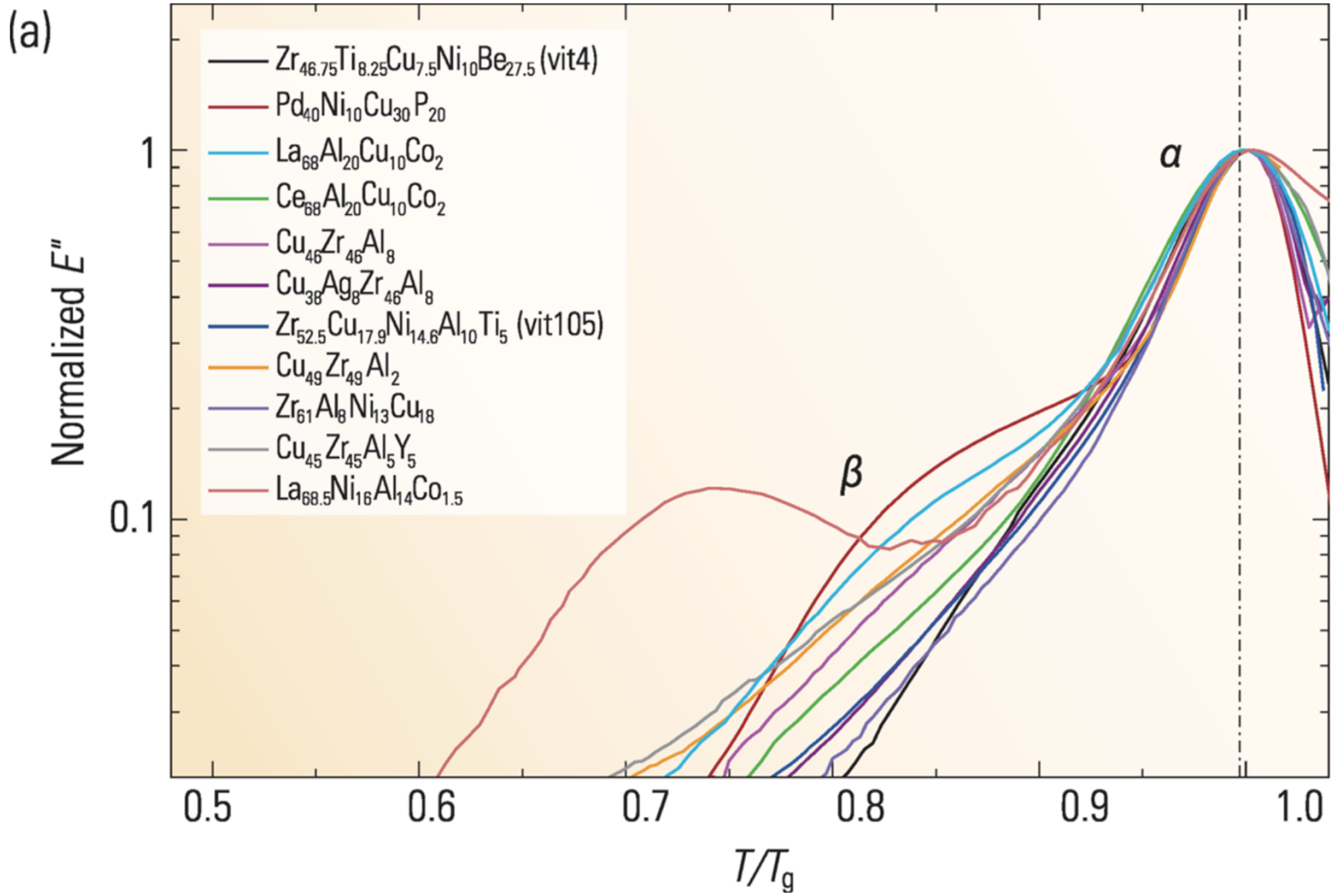

what is the slow-β relaxation, and where it comes from?

Under argument for 40 years

- Homogeneous process

  Williams & Watts, Trans. Faraday Soc. **67**, 1971 (1971).
  Fast, small-angle reorientations of all molecules.
  This motion is restricted to smaller amplitudes than the primary process.

- Inhomogeneous process "Islands of mobility"

  Johari & Goldstein, J. Phys. Chem. **53**, 2372 (1970).
  In regions of lower density "islands of mobility" molecules can partially reorient, giving rise to the process.

  ➢ **Johari-Goldstein relaxation**

Which is true for metallic glass?

structural inhomogeneity correlating to slow-β

- Weakly & strongly bonded regions

  Ichitsubo et al, PRL95, 245501 (2005)
  & JNCS357, 494 (2011)

  The size ξ of SBR
  ~ 4 nm in Pd-Ni-Cu-P
  ~1.5 nm in Zr-Al-Ni-Cu

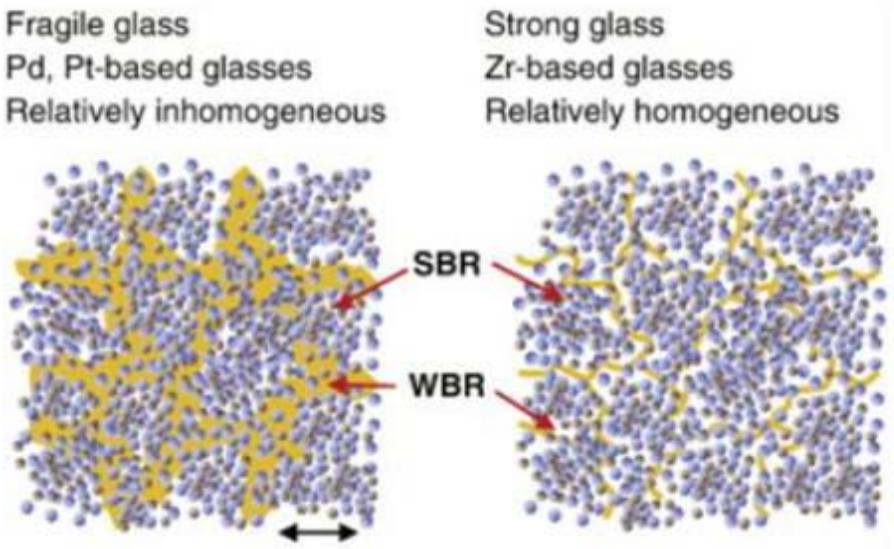

WBR, JG-relaxation & STZ

Wang et al, PRB75, 174201 (2007)
Local motion in the loser region below Tg
Q_β~ 28.4*RTg* (alloy dependence)

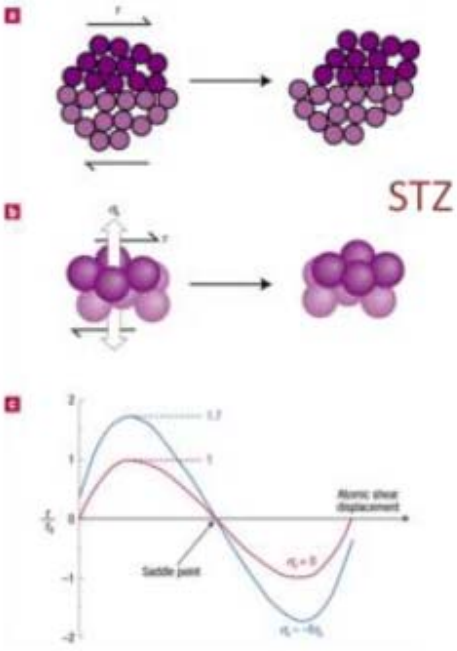

Wang et al, PRB81, 220201(R) (2010)
Slow β site ~ Shear Transformation Zone
by showing direct correlation between W_{STZ}~E_β.

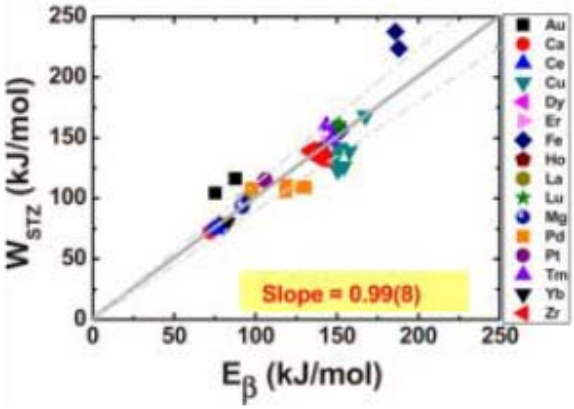

Relating β-relaxations to activation of STZs

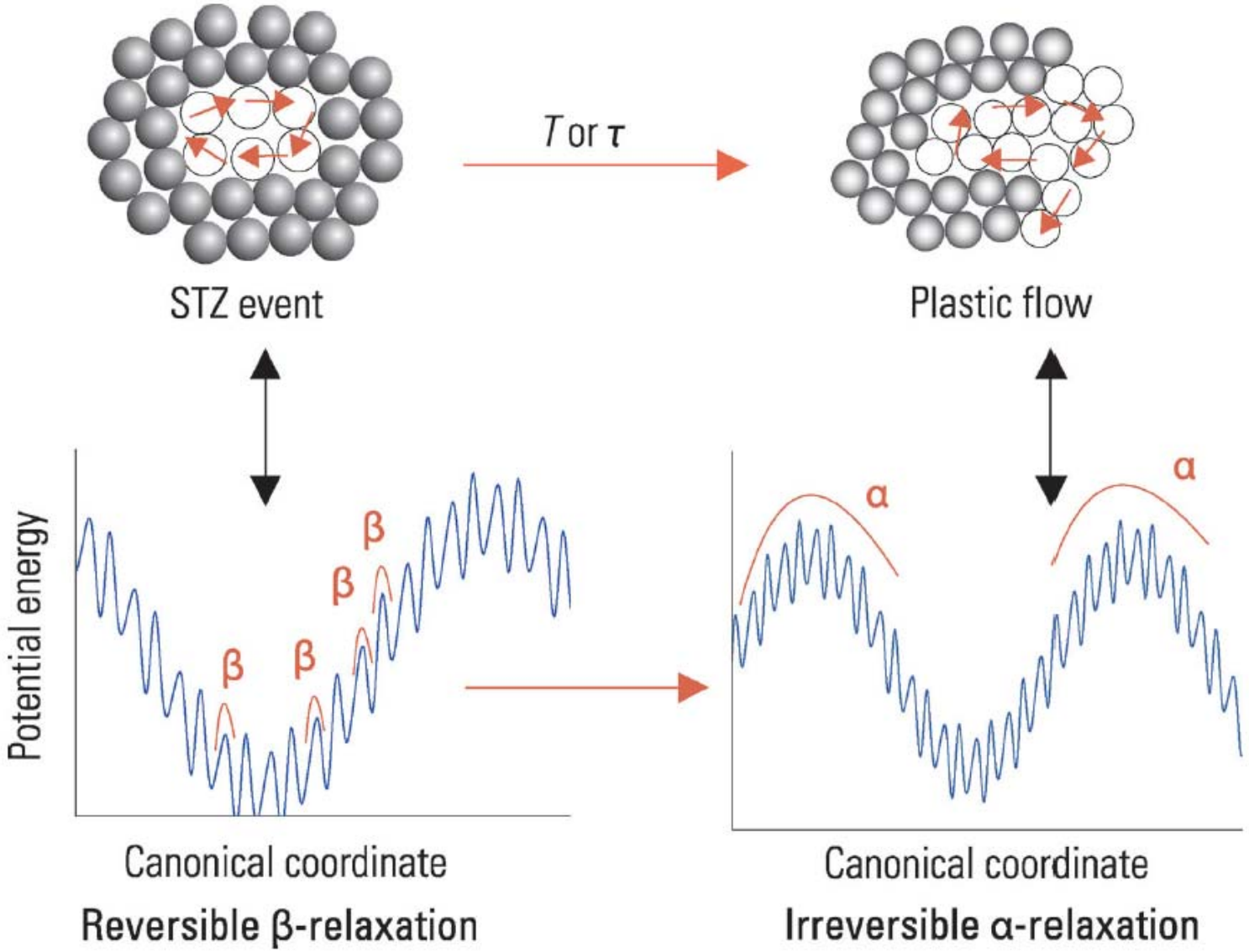

Yu, H. B., et al. (2014). "The β-relaxation in metallic glasses." *National Science Review* **1**(3): 429-461.

Alpha- & Beta-relaxation in metallic glasses

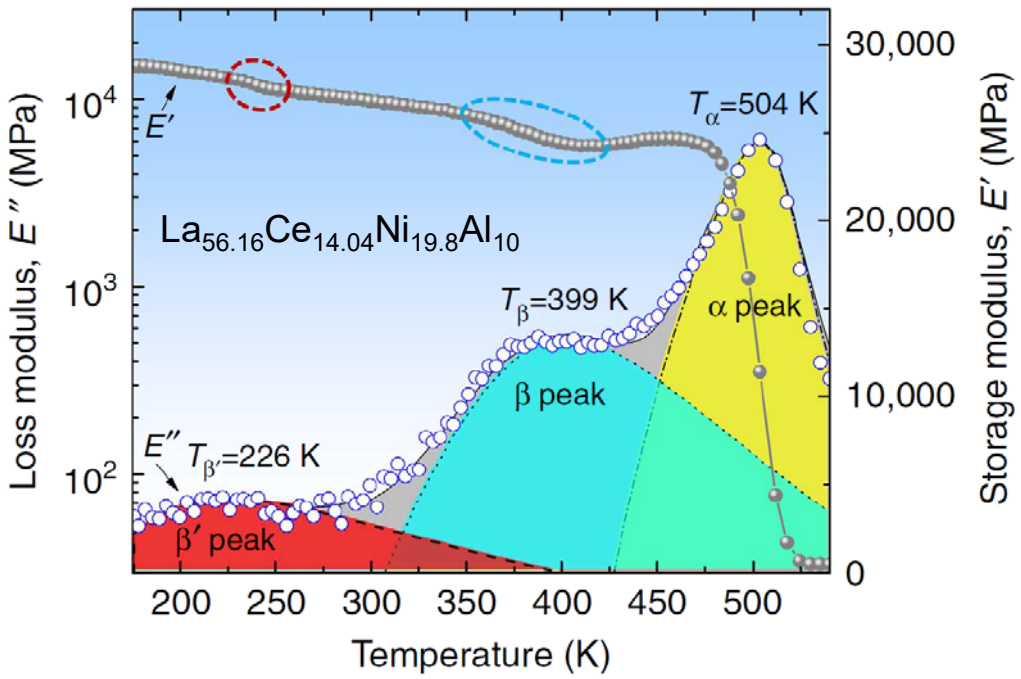

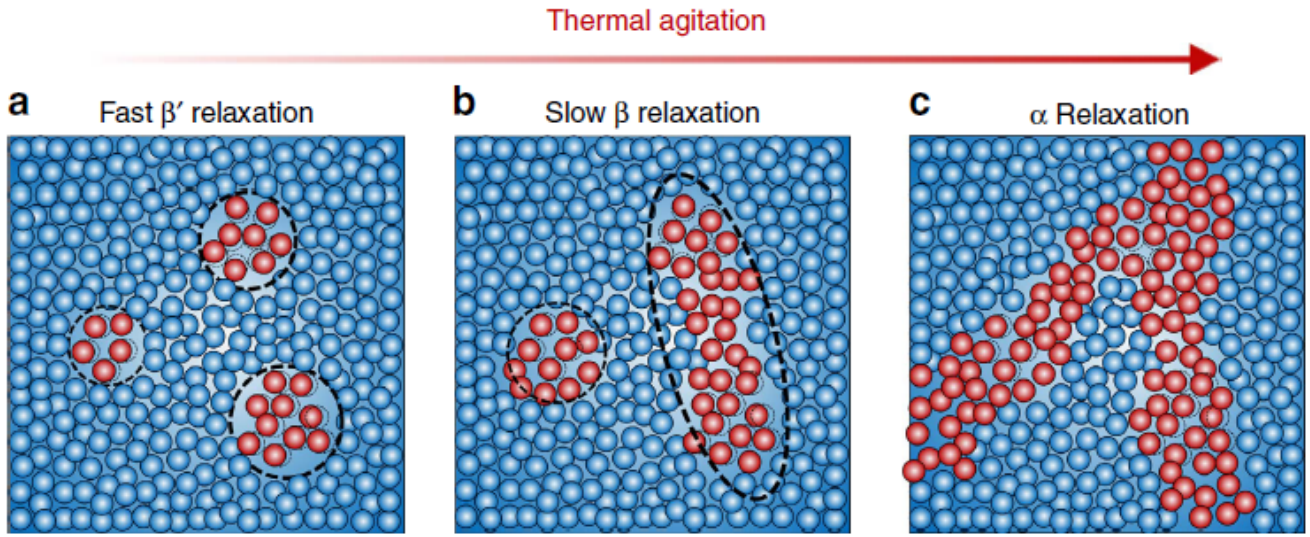

Wang et al., *Nature Commun.* **2015,** *6, 7876.*

How to measure the activation energy of β-relaxation

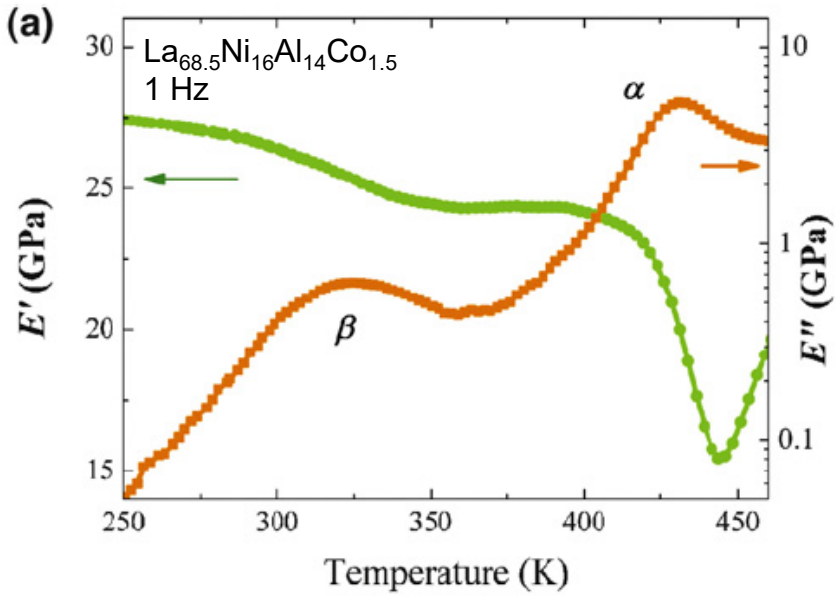

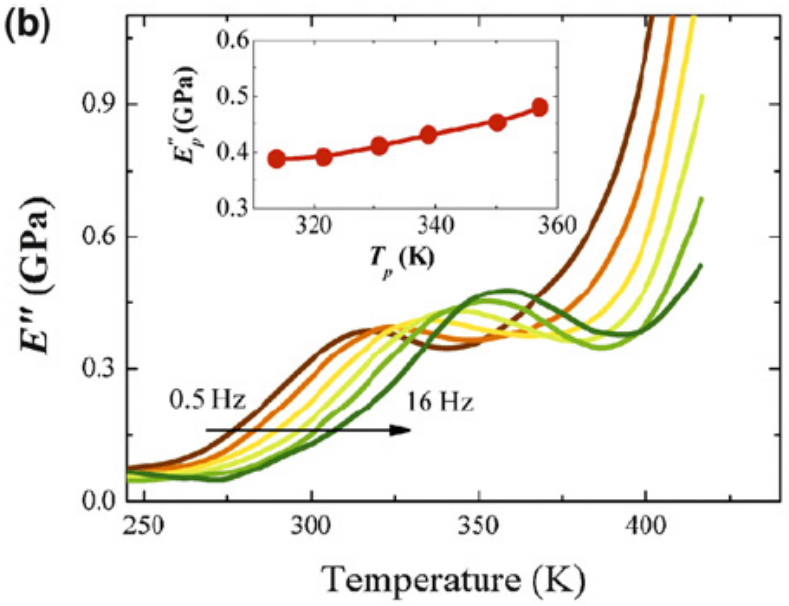

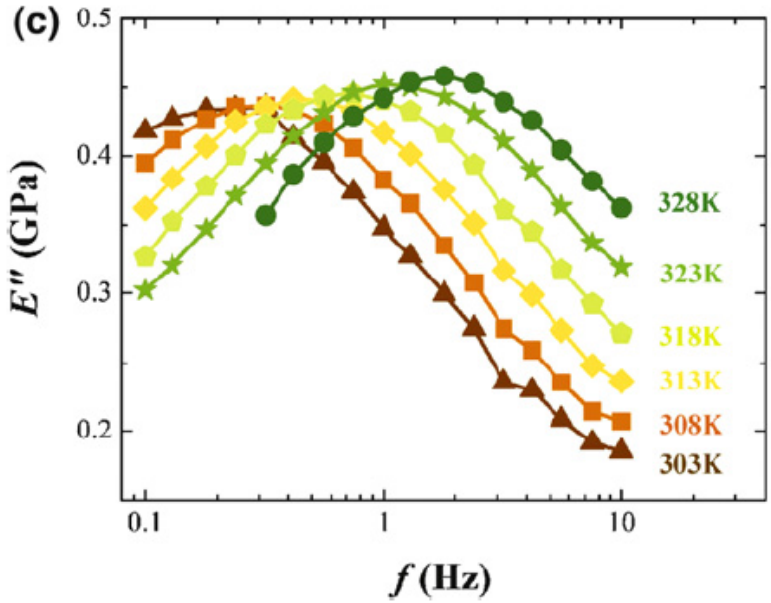

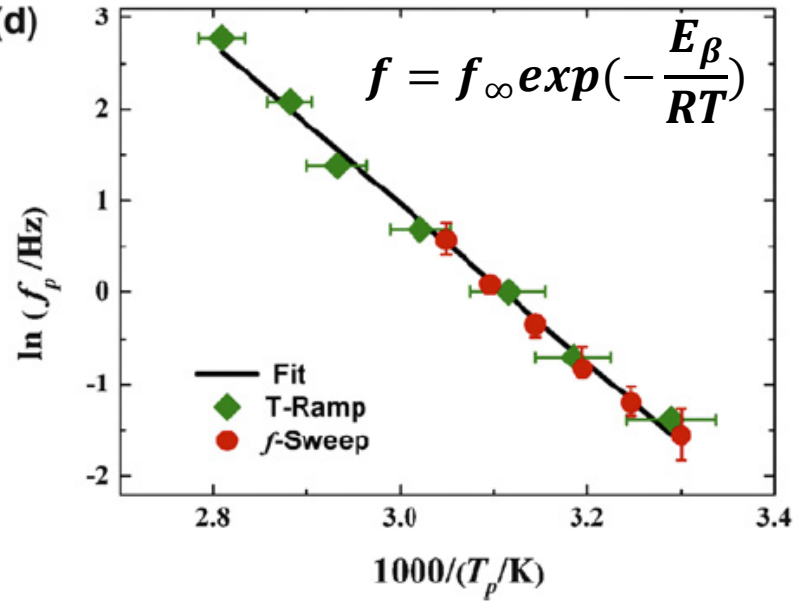

Yu et al., *Materials Today* **2013,** *16*, 183-191.

Activation energy of β-relaxation and Potential energy barrier of STZ

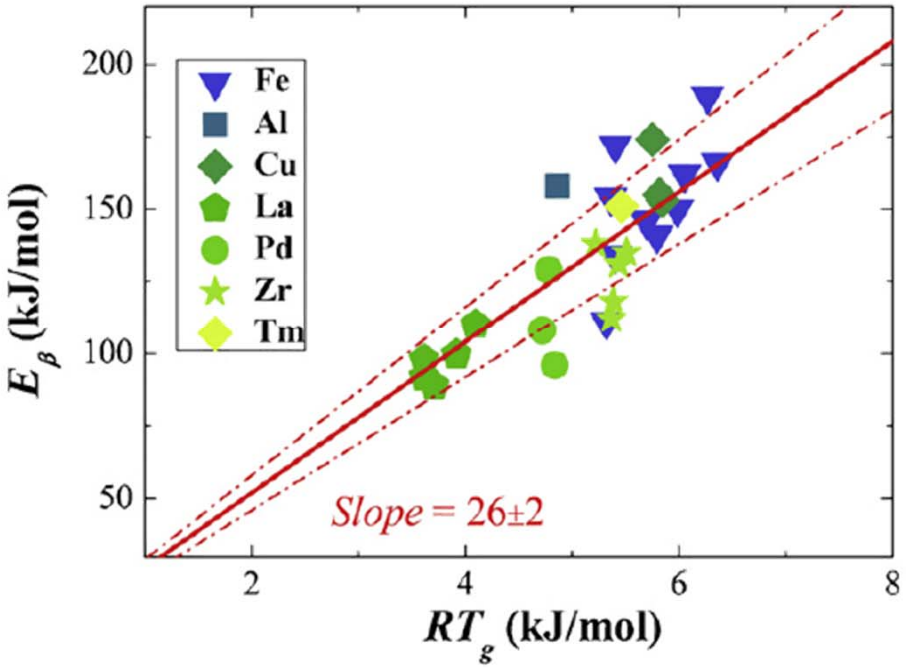

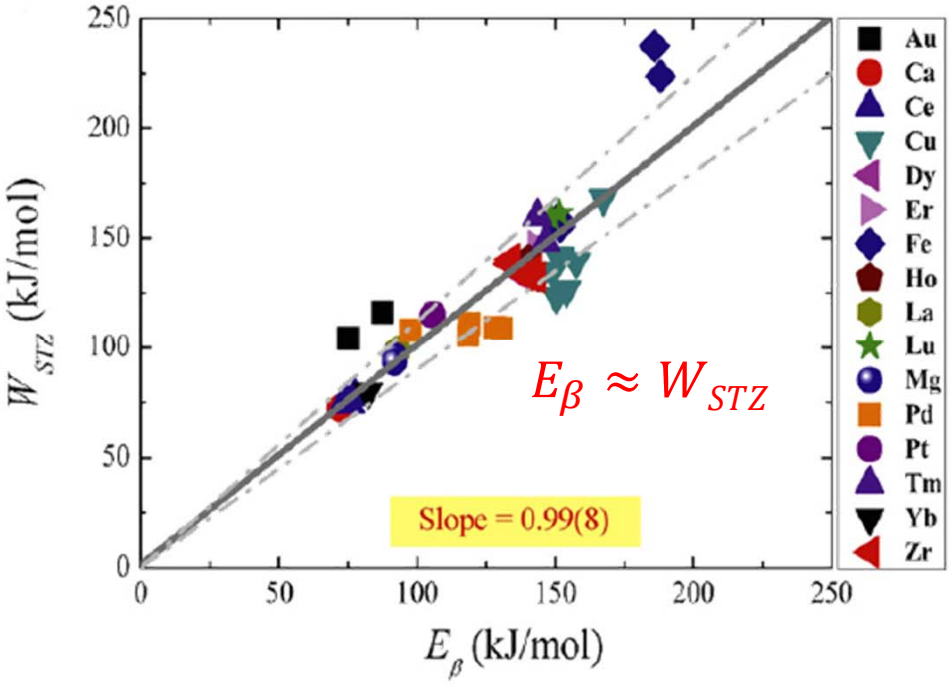

$$E_\beta = \sim 26RT_g$$

$$E_\beta = -RTln(\frac{f}{f_\infty})$$

$$W_{STZ} = \left(\frac{8}{\pi^2}\right) G{\gamma_c}^2 \zeta \Omega$$

Yu et al., *Materials Today* **2013,** *16*, 183-191.

Mechanically induced viscosity drop in metallic glass

Temperature-stress scaling for constant viscosity

$$\frac{T}{T_0(\eta)} + \left(\frac{\sigma}{\sigma_0(\eta)}\right) = 1$$

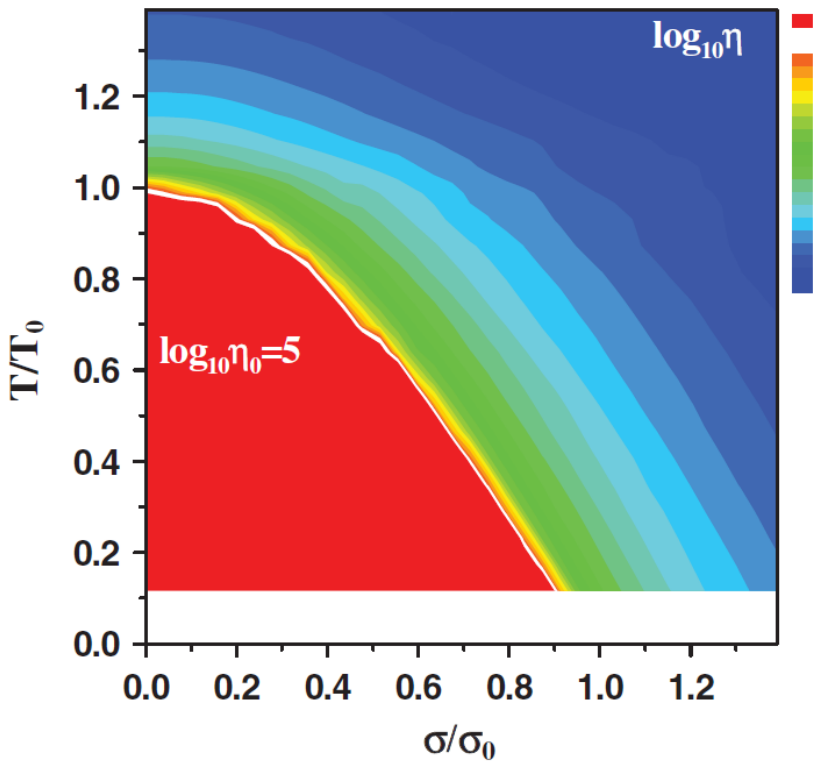

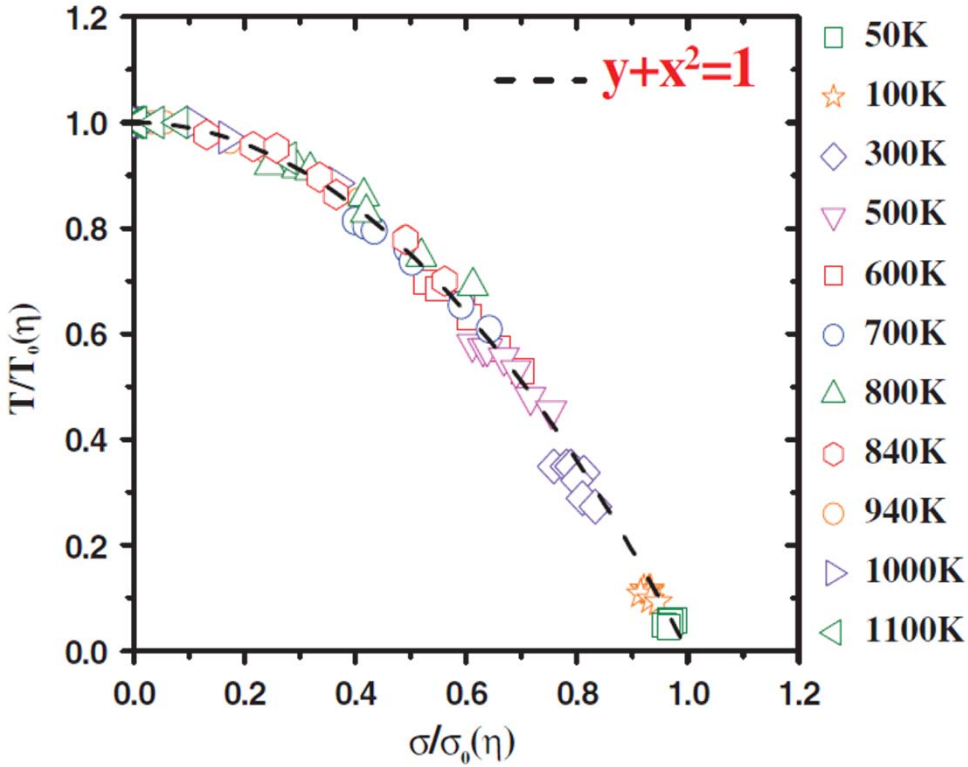

Applied shear stress has the equivalent effect as temperature in reducing the viscosity and inducing mechanical flow.

Guan et al., Phys. Rev. Lett. 104 (2010) 205701.

Microscopic and macroscopic flow regions in temperature domain

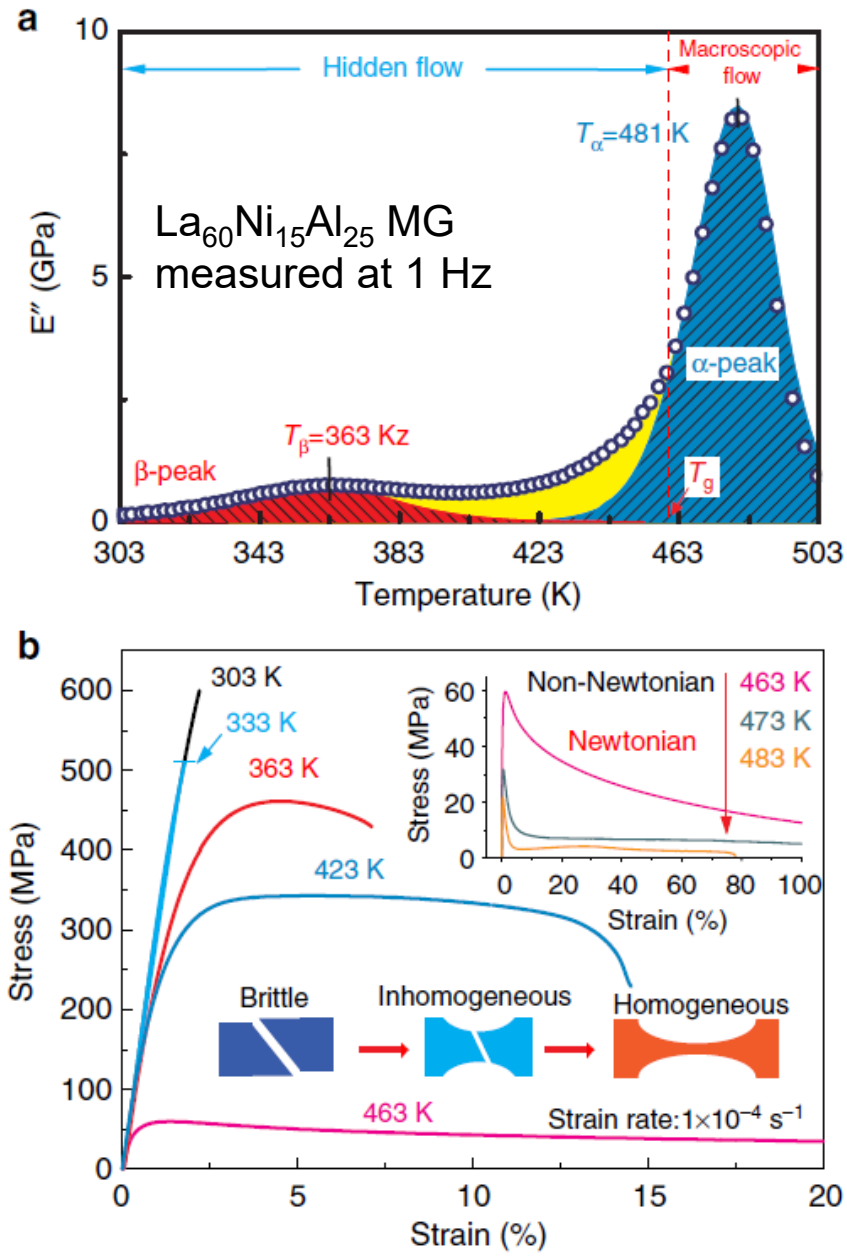

Correlations between deformation map and relaxation spectrum

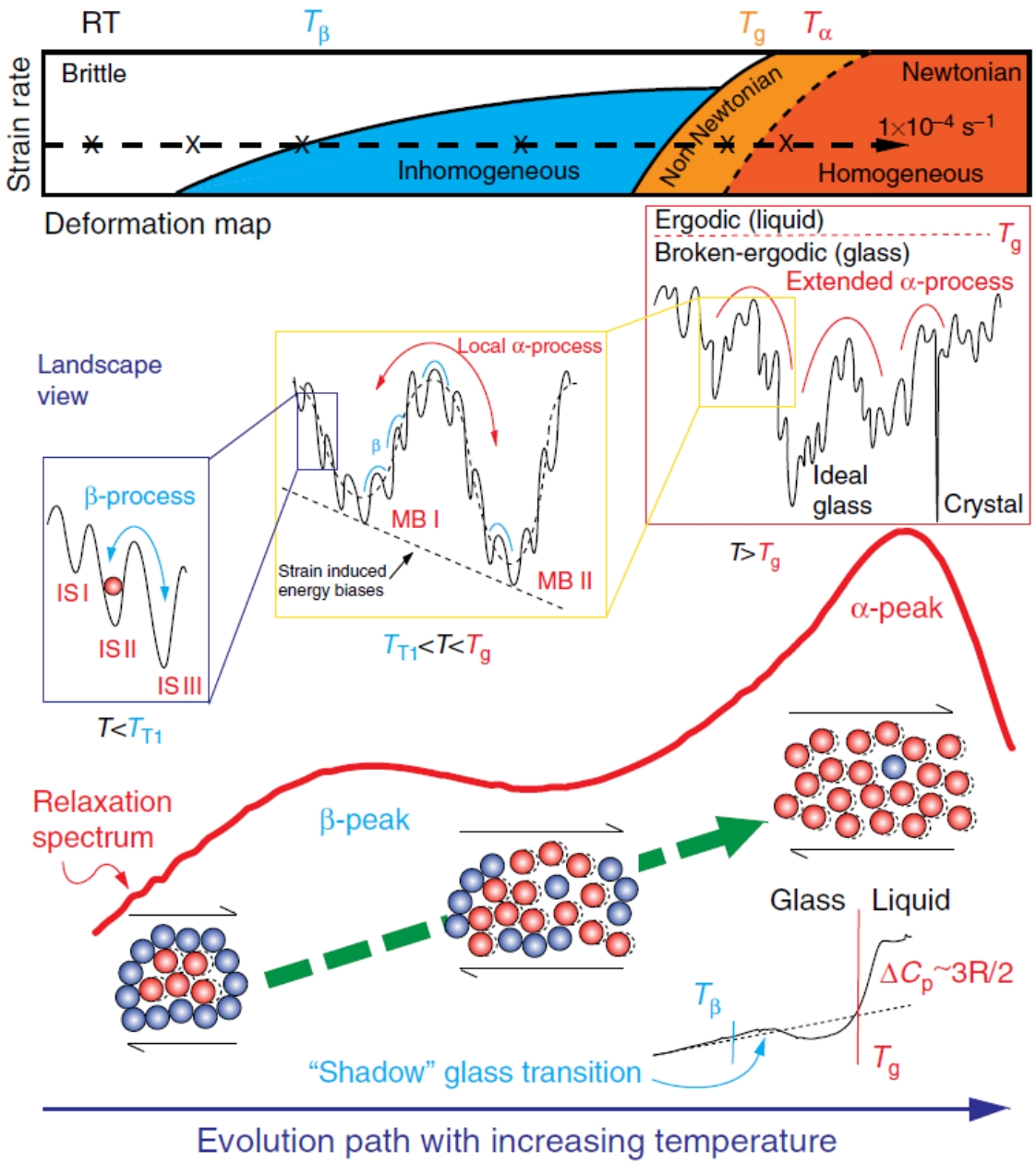

Wang et al., *Nature Commun.* **2014,** *5, 5823.*

* Electrical resistivity measurement during bending fatigue test

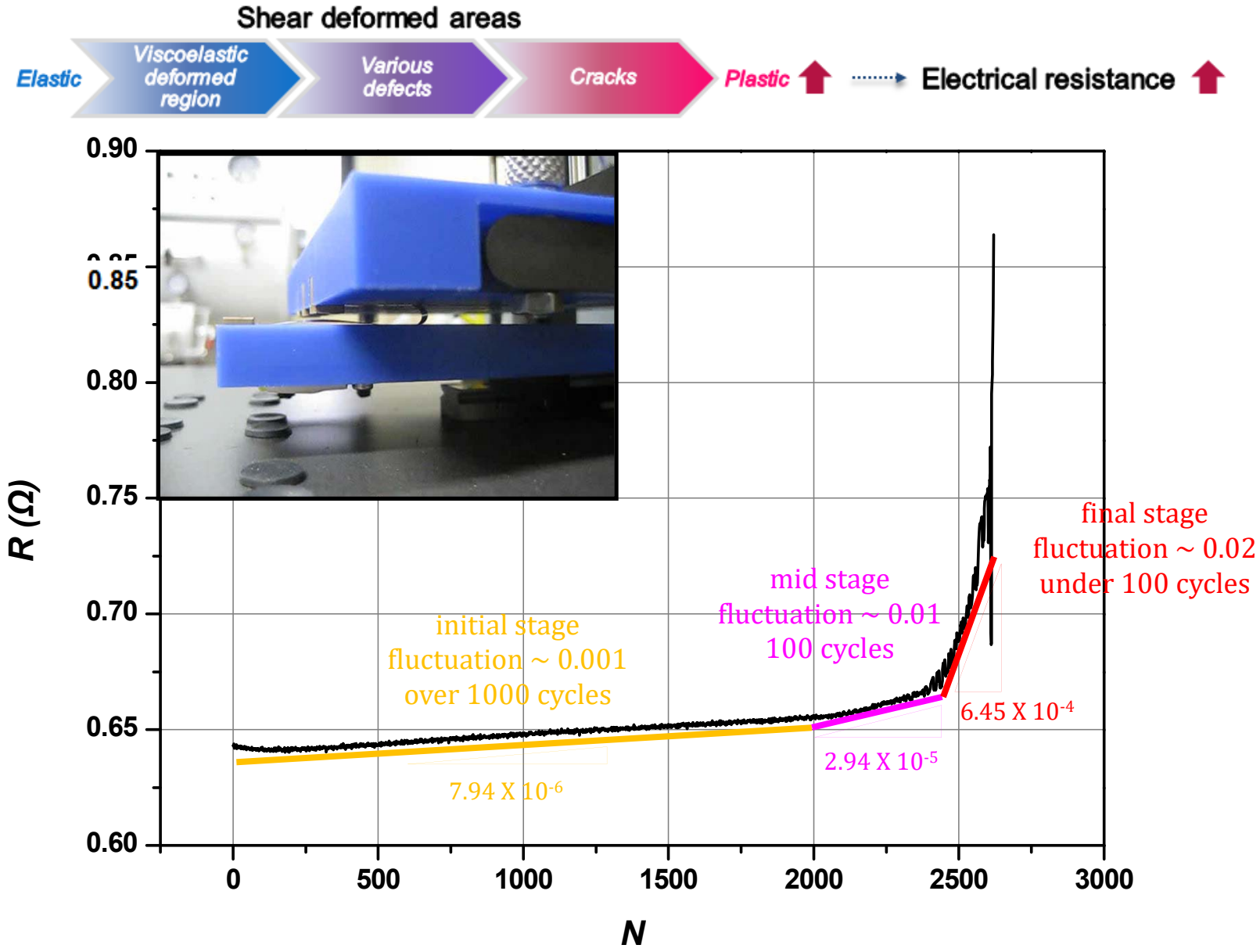

Zr50Cu40Al10 → 43% of the yield stress, 10^6 compressive load cycles

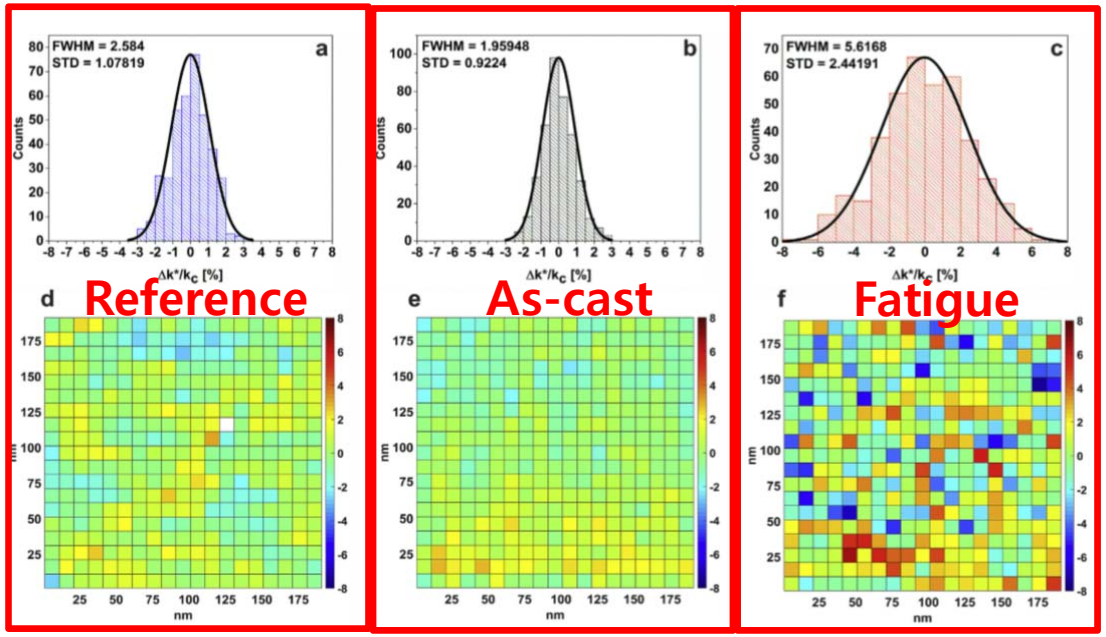

Fig. 2. (a–c) Distributions of the normalized contact stiffness, k^*/k_c, for Zerodur (a,d), the as-cast $Zr_{50}Cu_{40}Al_{10}$ (b,e) and the fatigued $Zr_{50}Cu_{40}Al_{10}$ (c,f). The distributions a-c were obtained from the 2D maps displayed in d-f.

Atomic force acoustic microscopy (AFAM)

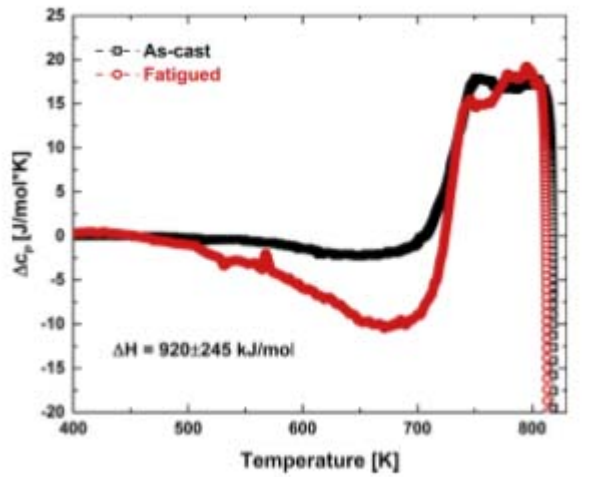

Fig. 5. (a) Heat release as a function of temperature during a DSC measurement of the as-cast and fatigued MG. A difference in stored enthalpy of 920 ± 245 J/mol is found.

Fatigue 발생시 elastic heterogeneity가 발생하게 되며 이에 따라 excess enthalpy의 storage가 발생하게 된다
--> Stress, Strain induced **rejuvenation 발생**

Ross, Perry, et al. "Linking macroscopic rejuvenation to nano-elastic fluctuations in a metallic glass." *Acta Materialia* 138 (2017): 111-118.

Various glass states of metallic glass

Nature Reviews Materials **1**, 16039 (2016)

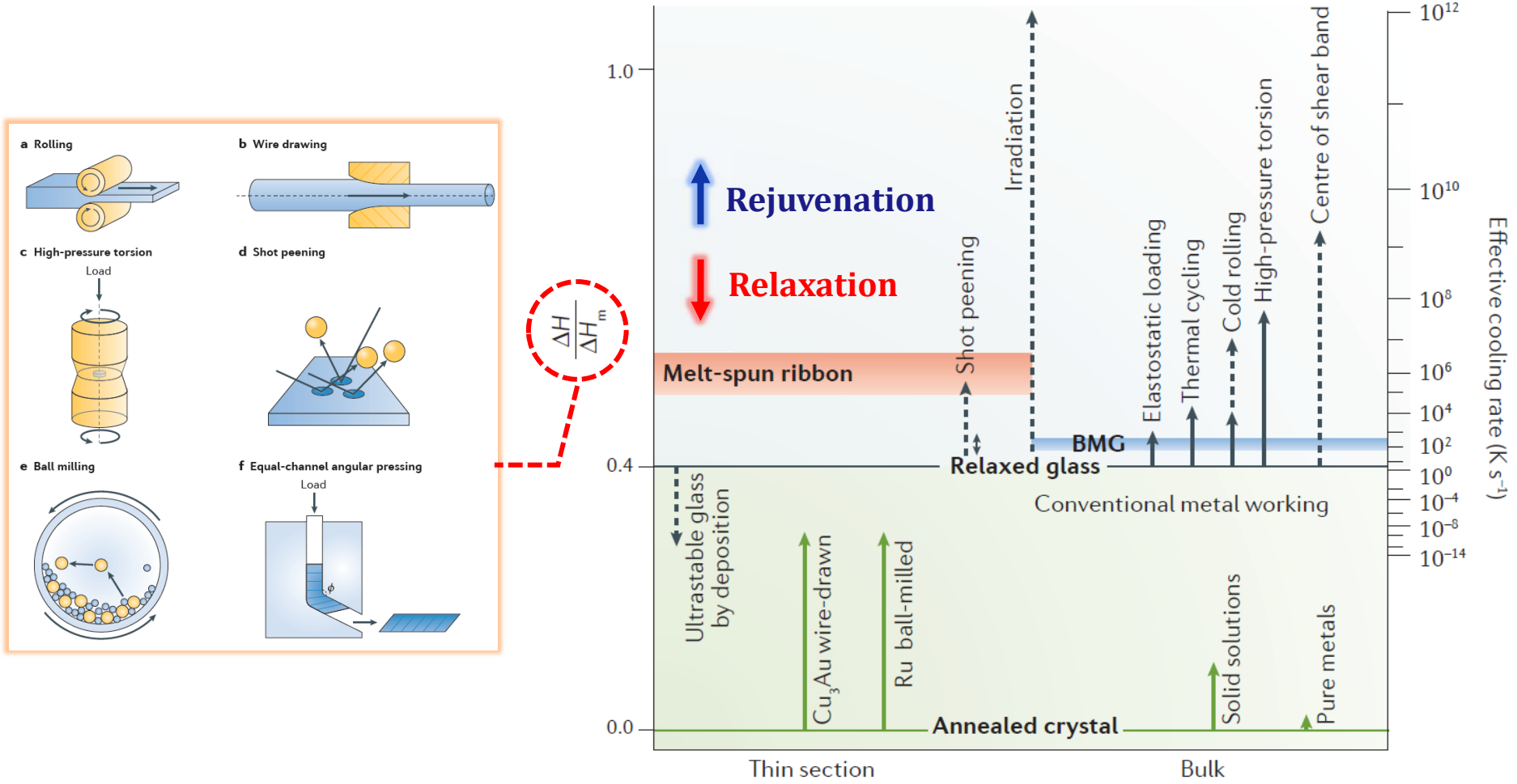

< Relative enthalpies of deformed metallic glass at RT>

- Metallic glass can form various glassy states depending on the cooling rate, thermomechanical process

Significance of studying (Rejuvenation)- (Relaxation)

Pan, J., et al. *Nature communications* 9.1 (2018): 560.

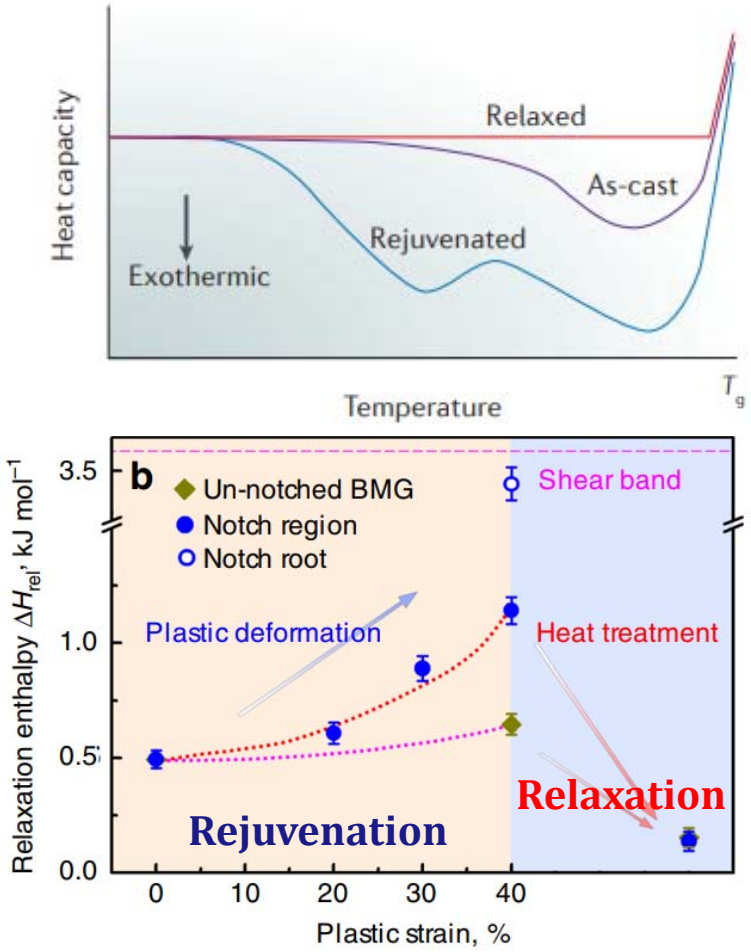

- Relaxation lower enthalpy, smaller volume

→ hard, brittle

- Rejuvenation brings material to higher E

→ Soft, less brittle state

- Relaxation (Sub-T_g annealing)

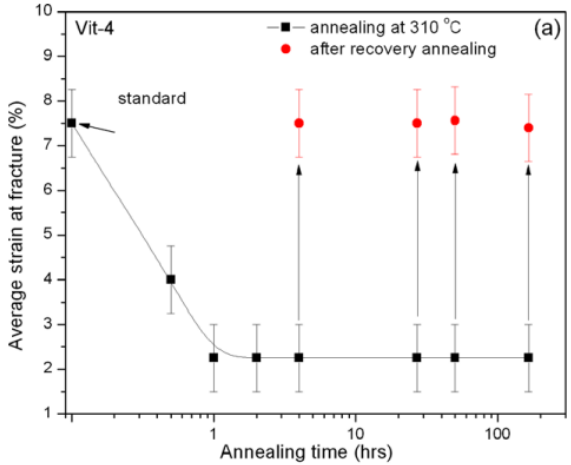

- Rejuvenation (77K-273K thermal cycling)

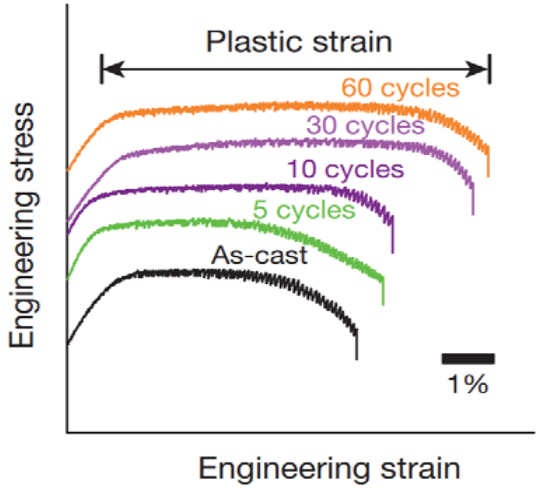

Reversible structural transition of MG : (Relaxation)-(Rejuvenation)

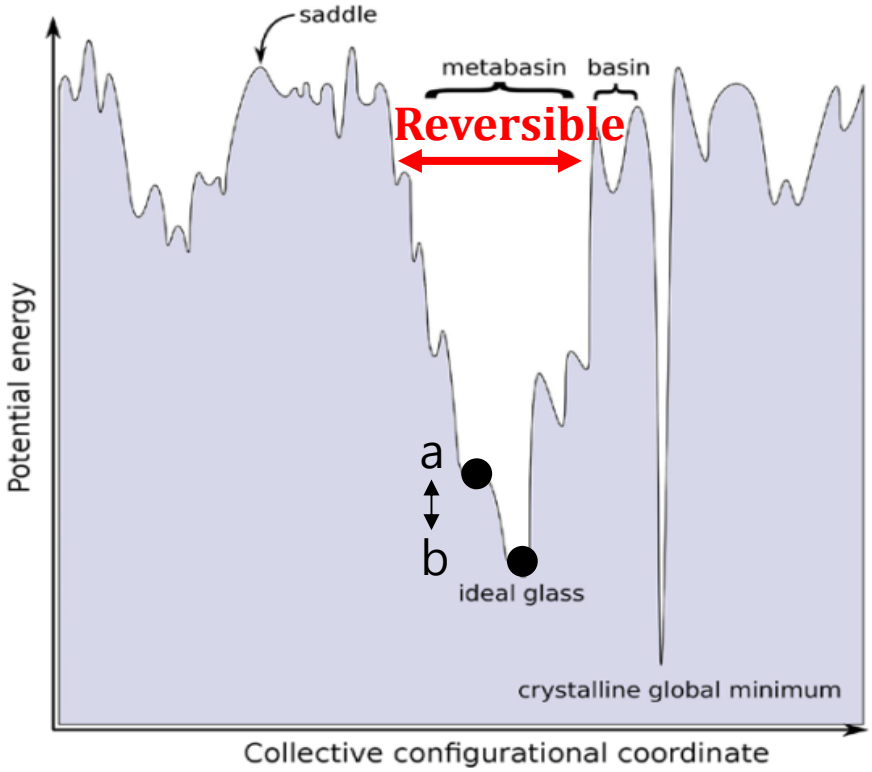

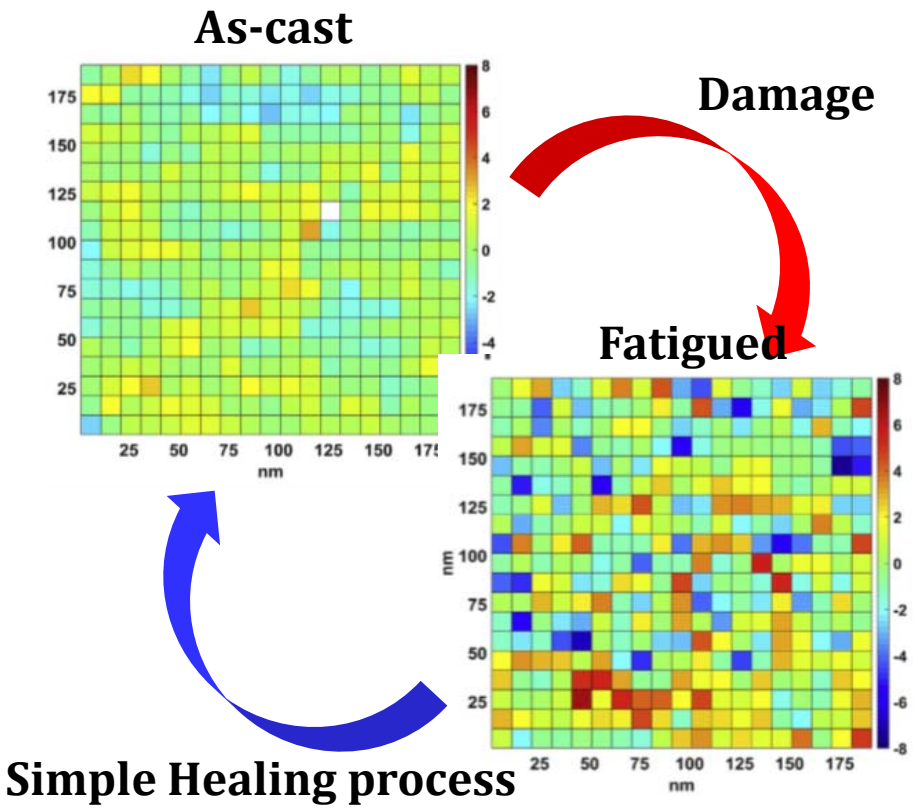

- One of the most big difference between (relaxation)-(rejuvenation) process of metallic glass with crystalline metal is that it is **reversible process**
- We can heal damage of metallic glass and even reset it to original structure
  → Under a clear understanding of **"structure"** and **"structure-property"** relationship